Science of the Total Environment 711 (2020) 134561

Contents lists available at ScienceDirect

Science of the Total Environment

journal homepage: www.elsevier.com/locate/scitotenv

A carbon mass-balance budget for a periglacial catchment in West Greenland – Linking the terrestrial and aquatic systems

Tobias Lindborg [a,b], Johan Rydberg [c,*], Eva Andersson [a], Anders Löfgren [d], Emma Lindborg [a], Peter Saetre [a], Gustav Sohlenius [e], Sten Berglund [f], Ulrik Kautsky [a], Hjalmar Laudon [b]

[a] Swedish Nuclear Fuel and Waste Management Co. (SKB), Box 3091, SE-169 03 Solna, Sweden
[b] Department of Forest Ecology and Management, Swedish University of Agricultural Sciences, SE-901 83 Umeå, Sweden
[c] Department of Ecology and Environmental Science, Umeå University, SE-901 87 Umeå, Sweden
[d] EcoAnalytica, Slalomvägen 28, SE-129 49 Hägersten, Sweden
[e] Geological Survey of Sweden (SGU), Box 670, SE-751 28 Uppsala, Sweden
[f] Hydroresearch AB, St. Marknadsvägen 15, SE-183 34 Täby, Sweden

HIGHLIGHTS

- How do dry periglacial conditions affect carbon pools and fluxes?
- A carbon mass-balance budget for an entire lake catchment in West Greenland.
- Terrestrial soils account for most of the long-term carbon storage.
- The lake is a source of CO_2 to the atmosphere, while hydrological export is limited.
- The dry conditions make this system different from other arctic environments.

GRAPHICAL ABSTRACT

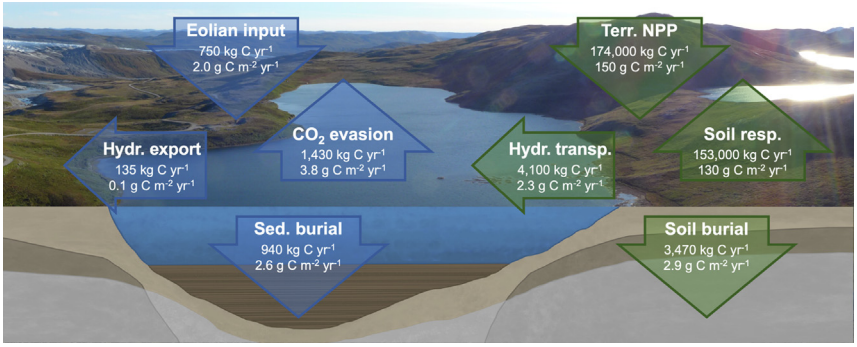

ARTICLE INFO

Article history:
Received 27 March 2019
Received in revised form 12 September 2019
Accepted 18 September 2019
Available online 18 November 2019

Editor: G. Darrel Jenerette

Keywords:
Carbon-budget
Whole catchment
Dry periglacial landscape
Terrestrial
Aquatic

ABSTRACT

Climate change is predicted to have far reaching consequences for the mobility of carbon in arctic landscapes. On a regional scale, carbon cycling is highly dependent on interactions between terrestrial and aquatic parts of a catchment. Despite this, studies that integrate the terrestrial and aquatic systems and study entire catchments using site-specific data are rare. In this work, we use data partly published by Lindborg et al. (2016a) to calculate a whole-catchment carbon mass-balance budget for a periglacial catchment in West Greenland. Our budget shows that terrestrial net primary production is the main input of carbon (99% of input), and that most carbon leaves the system through soil respiration (90% of total export/storage). The largest carbon pools are active layer soils (53% of total carbon stock or 13 kg C m^{-2}), permafrost soils (30% of total carbon stock or 7.6 kg C m^{-2}) and lake sediments (13% of total carbon stock or 10 kg C m^{-2}). Hydrological transport of carbon from the terrestrial to aquatic system is lower than in wetter climates, but the annual input of 4100 kg C yr^{-1} (or 3.5 g C m^{-2} yr^{-1}) that enters the lake via runoff is still three times larger than the eolian input of terrestrial carbon. Due to the dry conditions, the hydrological export of carbon from the catchment is limited (5% of aquatic export/storage or 0.1% of total export/storage). Instead, CO_2 evasion from the lake surface and sediment burial accounts for 57% and 38% of aquatic export/storage, respectively (or 0.8% and 0.5% of total export/storage), and Two-Boat Lake acts as a net source of carbon to the atmosphere. The limited export of carbon to

* Corresponding author.
E-mail address: johan.rydberg@umu.se (J. Rydberg).

https://doi.org/10.1016/j.scitotenv.2019.134561

downstream water bodies make our study system different from wetter arctic environments, where hydrological transport is an important export pathway for carbon.

1. Introduction

The low temperatures and frozen soils in arctic climates result in slow organic matter turnover and, thus, in a higher accumulation of organic matter per unit production as compared to other climatic settings (Hobbie et al., 2000; Mikan et al., 2002; Matzner and Borken, 2008; McGuire et al., 2009). However, the Arctic is currently warming, and is predicted to become even warmer in the future (Hanna et al., 2012; IPCC, 2013; Boberg et al., 2018), which has led scientists to suggest that arctic regions hold a key to understand the long-term effects of climate change on the global carbon cycle (Smol, 2012). This has induced a multitude of studies conducted across the Arctic looking at different aspects of carbon cycling, e.g., terrestrial primary production (e.g., Schuur et al., 2009; Eckhardt et al., 2019), soil organic carbon storage (e.g., Schuur et al., 2008; Palmtag et al., 2015; Siewert et al., 2015; Petrenko et al., 2016; Hugelius et al., 2013), heterotrophic soil respiration (e.g., Hollesen et al., 2011; Bradley-Cook and Virginia, 2016; Mikan et al., 2002; Eckhardt et al., 2019), carbon dioxide (CO_2) and methane (CH_4) evasion from surface waters (e.g., Lundin et al., 2015, 2016; Wik et al., 2016; Holgerson and Raymond, 2016; Northington and Saros, 2016; Rocher-Ros et al., 2017), the release of dissolved organic carbon (DOC) to surface waters (e.g., Frey and Smith, 2005; Lehmann-Konera et al., 2019), aquatic primary production (e.g., Whiteford et al., 2016; Mariash et al., 2018), and carbon burial in lake sediments (e.g., Anderson et al., 2009; Sobek et al., 2014).

Although these studies have significantly increased our understanding on specific aspects of the carbon cycle, there is a lack of studies that link the transport of carbon through the terrestrial and aquatic systems and look at the entire catchment using site-specific data. Previous landscape scale carbon budgets – i.e., studies looking at a spatial scale that include multiple catchments – either rely solely on aquatic data (e.g., Kling et al., 2000), or partially use data derived from other sites (e.g., Lundin et al., 2016). This lack of integration between the terrestrial and aquatic systems at a specific site reduce our ability to make reliable predictions of the net result of climate change on the carbon cycling (Lapierre and del Giorgio, 2012; Hanson et al., 2015; Solomon et al., 2015). Studies in the Arctic also tend to have a bias towards more humid areas, especially the areas around Abisko and Toolik Lake (Metcalfe et al., 2018). This makes it imperative to also study other types of arctic climates, e.g., the cold and dry conditions in West Greenland. Understanding cold and dry environments is not only interesting from the perspective of West Greenland. With increasing air temperatures many other Arctic areas are likely to become drier (Koenigk et al., 2013), or have already begun to do so (Smol and Douglas, 2007).

In this study, we present a carbon mass-balance budget for an entire lake catchment close to the inland ice-sheet in West Greenland. The data collection and most of the used data have previously been described and made available (but not interpreted or discussed) by Lindborg et al. (2016a,b). Here we use this empirical data set, which has been collected from both the terrestrial and aquatic parts of the catchment, together with a site-specific hydrological model (Johansson et al., 2015a) to calculate carbon pools and fluxes for the lake and its surrounding terrestrial catchment. The main hypothesis is that the dry and cold conditions result in a limited hydrological transport of carbon through the landscape as compared to other arctic or boreal sites. This would lead to a high accumulation of carbon in soils, reduce the hydrological link between the terrestrial and aquatic parts of the catchment, and give a low export of carbon from the catchment via the lake outlet. In addition, direct comparisons between the terrestrial and aquatic systems using data from a single catchment can answer the following questions: i) Are terrestrial soils or lake sediments the most prominent carbon sink in this cold and dry landscape? ii) Is eolian deposition or hydrological transport the most important transport pathway for carbon between the terrestrial and aquatic systems? iii) Is the aquatic ecosystem dependent on the supply of terrestrial carbon, and does the lake act as a sink or a source of carbon to the surroundings?

2. Methods

2.1. Field site

The climate in the Kangerlussuaq region, West Greenland, can be characterized as continental (Engels and Helmens, 2010). Annual average air temperatures measured in the settlement of Kangerlussuaq range from −9.1 to −0.3 °C (average −5.1 °C), with an observed increase in the annual average air temperature of approximately 2 °C between 1977 and 2013 (Hanna et al., 2012; Cappelen, 2016). The region is underlain by continuous permafrost – only interrupted by through taliks under large lakes – that extends down to 400 m depth (Harper et al., 2011), and the regional bedrock is dominated by tonalitic to granodioritic gneisses (van Gool et al., 1996).

The Two-Boat Lake catchment (TBL; Lat 67.125940 N Long 50.180370 W; Figs. 1 and 2) is situated 25 km northeast of Kangerlussuaq, about 500 m from the front of the ice sheet. The area is therefore by definition proglacial, but the absence of any hydrological connection with the ice sheet system and landscape maturity (up to 6800 years; Levy et al., 2012) also makes it possible to define the system as periglacial (Slaymaker, 2011). We refer to the site as the Two-Boat Lake, as established by Johansson et al. (2015a,b), Petrone et al. (2016) and Rydberg et al. (2016), but in other publications the lake has also been called SS903 (Sobek et al., 2014; Whiteford et al., 2016). The catchment area is 1.56 km^2, of which the lake covers 0.37 km^2 (Table 1). Deeper soils are dominated by till and glaciofluvial deposits, which are overlain by a 30–100 cm thick layer of eolian deposits mainly consisting of silt. Close to the lake and in wetter valleys the overlying eolian deposits can be characterized as peaty silt (Johansson et al., 2015a; Rydberg et al., 2016; Petrone et al., 2016). The catchment topography, active layer depth and lake bathymetry were described in detail by Petrone et al. (2016; Table 1).

Terrestrial vegetation can be divided into dwarf shrub, meadow, dry grassland and wetland communities (Lindborg et al., 2016a). Areas with dwarf shrub are dominated by dense stands of *Betula nana* (Linnaeus) and/or *Salix* spp. The meadow and dry grassland vegetation types lack woody plants. Meadows consist mainly of grasses and herbs, while dry grassland is dominated by *Kobresia* and *Carex*. Wetland communities are dominated by *Carex* with a bottom layer of bryophytes, e.g., *Sphagnum* (Lindborg et al., 2016a). There are no trees in the catchment, and shrubs rarely exceed a height of 0.5 m.

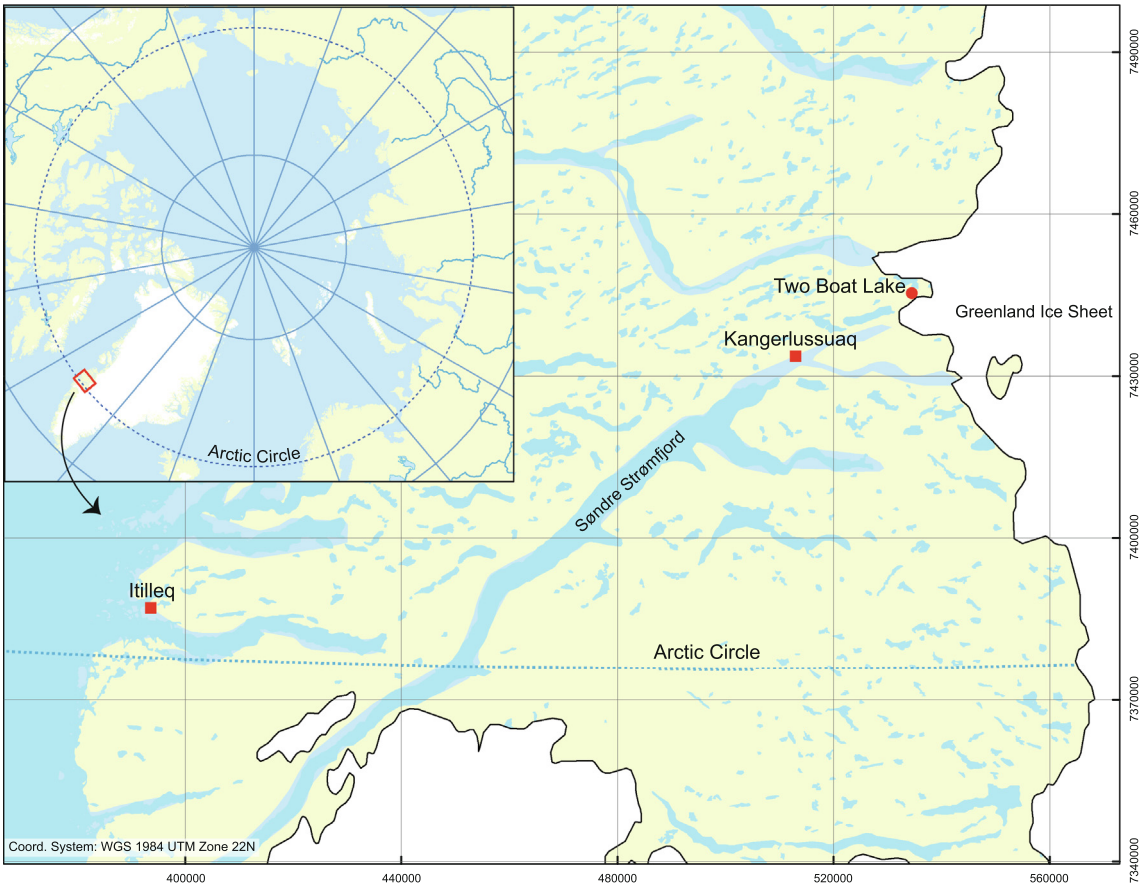

Fig. 1. Map of West Greenland and location of the TBL catchment. Modified after Johansson et al. (2015b).

Local annual precipitation at the TBL catchment varies between 163 and 366 mm (2011–2018), with an average of 269 mm (Johansson et al., 2015a; Johansson, 2019). The initial phase of the hydrologically active period – i.e., when the active layer begins to thaw in May–June – accounts for about 40% of the annual water input to the lake. However, there are no permanent streams in the catchment and lake-water outflow occurs only occasionally during spring thaw and autumn rains (Table 1; Johansson et al., 2015a,b). In most years the water balance is slightly positive, but during dry years it turns negative resulting in a lowering of the lake level (Johansson et al., 2015a,b). Over the last 30-year period the modelled average annual lake outflow represents 0.1% of the lake volume (Johansson et al., 2015a).

The lake itself has maximum and average water depths of 29.9 m and 11.3 m, respectively, and the lake volume has been estimated to 4.25 Mm^3 when the lake water level reaches the threshold where outflow occurs (Table 1). Ice-out occurs in mid-June and the length of the ice-free season – determined from time-lapse photos (2011–2013) – varied between 125 and 135 days (Johansson et al., 2015b). Total Organic Carbon (TOC) and dissolved organic carbon (DOC) are on average 8.7 ± 0.7 and 8.5 ± 0.4 mg L^{-1} (Lindborg et al., 2016a), respectively (2010–2018), and water transparency (measured as Secchi depth) was about 15 m in 2010 (Lindborg et al., 2016a; Wetzel, 2001). The lake bottom can be divided into shallow wind exposed areas with non-vegetated rocks and boulders, areas with soft sediments covered by aquatic vegetation (down to between 14 and 16 m water depth), and deeper areas with soft sediments without any vegetation (Lindborg et al., 2016a). No fish were found in the lake, but tadpole shrimps (*Lepidurus arctica,* Pallas) and fairy shrimp *(Branchinecta paludosa*, Müller*)* are common (Lindborg et al., 2016a). When compared to other lakes in the region (Ryves et al., 2002; Sobek et al., 2014), TBL is only slightly larger and deeper than the average lake in the region, and the water chemistry (pH, TOC, Total nitrogen and Total phosphorus) is close to the regional average, although the conductivity is much lower than in the oligo-saline lakes located further from the front of the ice sheet (Supporting information Table 1; Whiteford et al., 2016).

2.2. Field experiment design

The basis for this study is a coupled terrestrial-aquatic conceptual model where the landscape is divided into pools (e.g., terrestrial biota, active layer soils, permafrost soils, water column, aquatic biota, lake sediments), which are linked through a number of flow paths (Fig. 3). The approach is comparable to those previously used to develop separate aquatic and terrestrial ecosystem models in boreal landscapes (Andersson and Sobek, 2006; Löfgren et al., 2006). The carbon data for each pool was then used together with information on the volume of each pool (Petrone et al., 2016) and hydrological flows (Johansson et al., 2015a,b) to construct a simple carbon mass-balance budget for the entire catchment (Fig. 3).

2.3. Sampling

Sampling of terrestrial and aquatic biota, waters, soils and sediments was carried out during the period 2010–2018 (Fig. 2). Further details regarding sampling and analysis can be found in Lindborg et al. (2016a) and all data collected prior to 2016 is available in the corresponding database (Lindborg et al., 2016b; Supporting information Table 2). Below follows a summarized

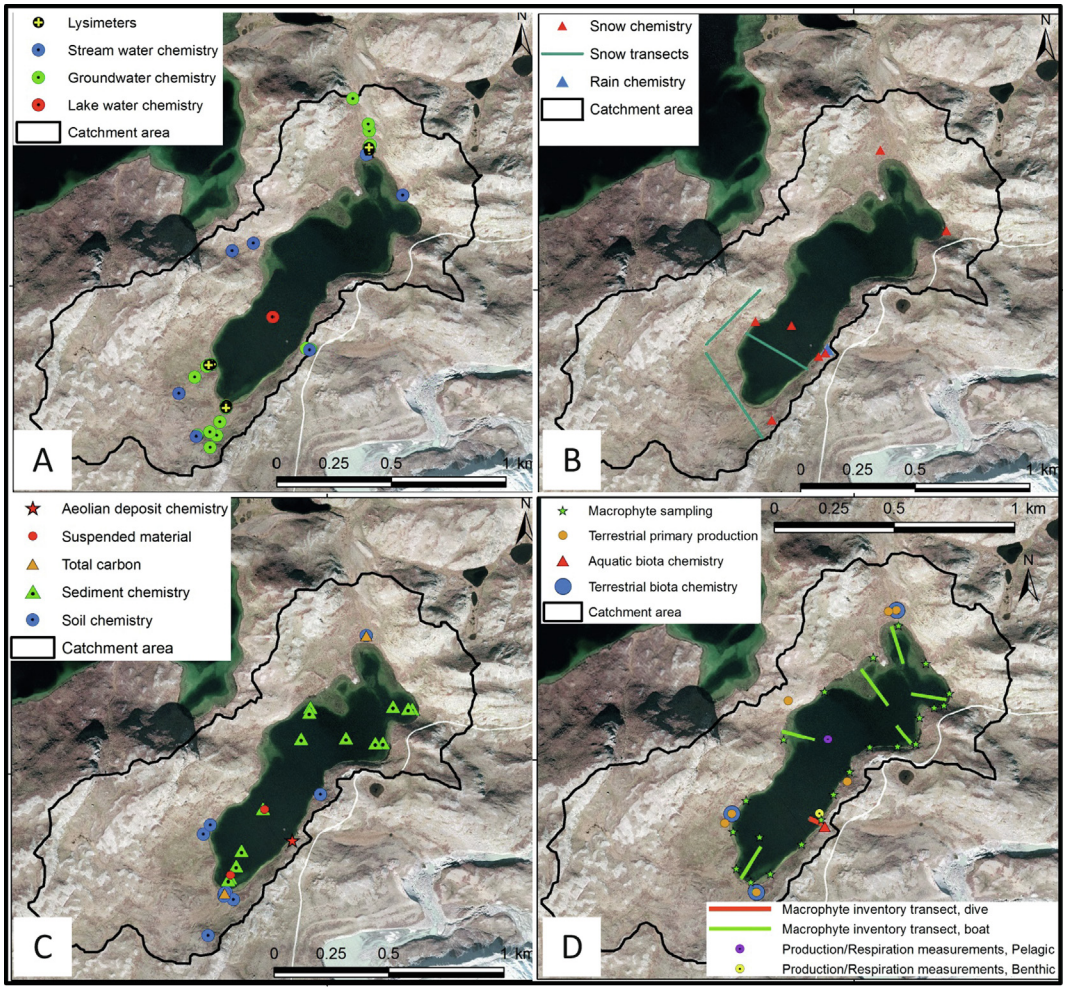

Fig. 2. Map of TBL catchment and sampling points. Modified after Lindborg et al. (2016a). For data and sampling coordinates, see Lindborg et al. (2016b).

description of the methods used in this study, the assumptions that were made, and how the data were treated and used when calculating pools and fluxes.

2.3.1. Sampling atmospheric deposition

Filtered (0.45 μm) rain samples (n = 2) and fresh snow samples – without any visible eolian dust – were collected using plastic containers (n = 4; Lindborg et al., 2016a). In late winter old snow packs (n = 2) containing extensive eolian dust were collected from sheltered locations representative for areas with continuous accumulation of snow and eolian material (under the assumption that snow and eolian material have a similar pattern of accumulation).

2.3.2. Terrestrial ecosystem sampling

For each of the main vegetation types (dwarf shrub, meadow, dry grassland and wetland) above-ground and litter biomass were determined through destructive sampling (3 plots per vegetation type; Lindborg et al., 2016a). Soil organic carbon (SOC) and root content for each of the vegetation types were determined from short (12 cm) or long (40–110 cm) soil cores (2–7 per vegetation type). The two longest soil cores, taken in wetland vegetation type, extended down into the permafrost.

2.3.3. Soil and stream water sampling

Soil water samples were collected from lysimeter installations in the wetland areas (n = 18), while both filtered (0.45 μm) and unfiltered surface water was sampled from temporary streams flowing into the lake (n = 29; Lindborg et al., 2016a; in 2017 and 2018 only filtered samples were collected).

2.3.4. Lake ecosystem sampling

Lake water for TOC, DOC and DIC analysis was sampled from shallow (3–5 m depth) and deep water (25 m). Both filtered (0.45 μm) and unfiltered samples were collected (in 2018 only filtered samples were collected). Depth profiles of oxygen, temperature and pH were measured at the lake center using a Troll 9500 multi-parameter probe.

Biomass estimates for benthic vegetation were made on three occasions from areas with soft sediments down to 16.3-m water depth (both wind-sheltered and less wind-sheltered locations). Benthic vegetation from different water depths was sampled destructively from square 0.12-m^2 (n = 27) or circular 0.08-m^2 plots (n = 9; Lindborg et al., 2016a). Benthic macro fauna was sampled quantitatively from areas with soft sediments between 3 and 27 m water depth using an Ekman 'Grab' (16 × 16 cm; n = 18), and benthic bacteria was sampled from two depths (16 and 29.8-m water depth; n = 12) using a gravity corer (8.3 cm diameter; Renberg and Hansson, 2008). Quantitative samples for phytoplankton and bacterioplankton were collected from both the epilimnion (0.5, 5 m and 12 m; n = 15) and hypolimnion (25 m; n = 9) using a Ruttner sampler. Zooplankton were sampled quantitatively by filtering 6-L water samples from the epilimnion (5 m; n = 3) and hypolimnion (25 m; n = 1) through a 65 μm mesh (Lindborg et al., 2016a).

Table 1
Long term water budget and geometrical data for the TBL catchment. Data are based on the water budget from Johansson et al. (2015a), time lapse cameras (lake ice in/out) and geometrical data from Petrone et al. (2016).

	Value
Terrestrial system	
P	348000 m^3 yr^{-1}
ET	257500 m^3 yr^{-1}
Total runoff to lake	106300 m^3 yr^{-1}
Runoff related to snowmelt	55200 m^3 yr^{-1}
Limnic system	
P	100100 m^3 yr^{-1}
E	179100 m^3 yr^{-1}
Lake water outflow	5300 m^3 yr^{-1}
Groundwater recharge to talik	6300 m^3 yr^{-1}
Lake water residence time	47 yr
Ice in	Early-Oct
Ice out	Mid-June
Geometrical parameters	
Catchment area	1.56 km^2
Terrestrial catchment area	1.18 km^2
Lake area	0.38 km^2
Lake area, <16-m deep	0.22 km^2
Lake area, >16-m deep	0.16 km^2
Lake volume[1]	4250000 m^3
Lake volume, <14-m deep	3178000 m^3
Lake volume, >14-m deep	1072000 m^3
Lake maximum depth	29.9 m
Lake mean depth	11.3 m
Active layer depth[2]	0.48–0.8 m
Elevation, maximum	516 m a.s.l.
Elevation, lake surface[1]	336.7 m a.s.l.

[1] Lake level and lake volume is the maximum values when the lake level was close to the threshold when outflow occurs (Sept. 2010). Lake water level, and thus the lake volume, varies between years, and the minimum volume and lake level during the study period was 4,140,000 m^3 and 336.4 m a.s.l., respectively (Johansson et al., 2015a).
[2] Bedrock outcrop areas excluded.

Pelagic gross primary production ($GPP_{Pelagic}$) was estimated by correcting the production of oxygen in light incubations for the consumption of oxygen in dark incubations (Wetzel and Likens, 1979). Quartz glass bottles were incubated for about 4 h around noon along depth profiles (0.1, 0.25, 0.5, 1, 2, 3, 5, 10, 15 and 20 m depth) on two sunny days (16 June 2012 and 22 August 2013; Lindborg et al., 2016a). Benthic net primary production ($NPP_{Benthic}$) was estimated from measurements of oxygen production/consumption in clear plexiglass chambers placed on the lake bottom between the 16–17 June 2013 and 20–21 August 2013 (because no dark incubations were made no benthic GPP estimate could be calculated). Oxygen was measured using a Hanna oxygen meter (resolution 0.01 mg O_2 L^{-1}).

2.3.5. Sediment sampling

In 2012, 13 surface-sediment cores (23–40 cm long) from four depth transects were collected using a gravity corer (Lindborg et al., 2016a). Sampling locations were selected to provide an adequate representation of vegetated and non-vegetated areas, different locations in the lake basin, as well as, different water depths.

2.4. Analysis

TOC and/or DOC in all water samples (rain, snow, soil-, stream- and lake-water) were analyzed by thermal combustion following acidification (to remove DIC) in a TC/TIC/TOC-analyzer (Lindborg et al., 2016a). DIC in water samples was analyzed by acidifying the samples and detecting the produced CO_2 (Lindborg et al., 2016a). On all occasions when both TOC and DOC were analyzed in water samples that were collected at the same time (n = 4) the difference between TOC and DOC were less than 0.1 mg L^{-1}, therefore POC was assumed to be negligible and DOC concentrations have been considered to represent TOC in our calculations.

All soil samples were analyzed for loss-on-ignition (LOI) at 550 °C. The LOI was then converted to SOC by using a conversion factor of 0.58 (van Bemmelen, 1890). All lake sediment samples and a smaller number of soil samples (n = 18) were analyzed for organic carbon using elemental analysis (Flash EA 2000, Thermo Fisher Scientific; Lindborg et al., 2016a). The ratio between organic carbon and LOI in the soil samples where both OC and LOI was analyzed ranged from 0.29 to 0.88 (average 0.54), which shows that the van Bemmelen factor works reasonably well also for this system. The carbon content in roots was converted to carbon by using a dry-weight-to-carbon conversion factor of 0.5 (Löfgren, 2010).

Phytoplankton and zooplankton were determined using an inverted phase-contrast microscope (Lindborg et al., 2016a). The phytoplankton carbon content was estimated by assuming a wet weight of 1 g cm^{-3} biovolume and using taxa-specific carbon-content conversion factors presented by Olrik et al. (1998). For zooplankton, the carbon content was estimated by using length-to-dry weight conversion factors (Johansson et al., 1976; Ruttner-Kolisko, 1977), and assuming a dry-weight-to-carbon conversion factor of 0.48. For benthic and pelagic bacteria, the volume was first determined by measuring the size of at least 100 cells. Then the bacteria dry weight was calculated according to Eq. (1).

$$\text{Dry weight} = 435 \times \text{biovolume}^{0.86} \quad (1)$$

with dry weight in grams and volume in cubic centimeters (Loferer-Krössbacher et al., 1998). Finally, the carbon content was estimated by assuming a dry-weight-to-carbon conversion factor of 0.5 (Kemp et al., 1993). In aquatic macrophytes the carbon content was calculated from the total mass by assuming a dry-weight-to-carbon conversion factor of 0.4 (Kautsky, 1995). For the benthic fauna, it was assumed that the dry weight was 20% (Kautsky, 1995) of the wet weight, and the carbon content was calculated by assuming a dry-weight-to-carbon conversion factor of 0.3 (Kautsky, 1995).

Carbon-14 (^{14}C) was analyzed using accelerated mass spectroscopy (AMS; Lindborg et al., 2016a). Radiocarbon ages were then converted to calibrated ages using the InterCal 13.14C (Hua et al., 2013; Reimer et al., 2013) in the online version of Oxcal 4.2 (https://c14.arch.ox.ac.uk; Bronk Ramsey, 2009). Lead-210 (^{210}Pb) was analyzed by measuring the activity of its daughter isotope polonium-210 (^{210}Po) by means of alpha spectrometry (Appleby, 2008; Lindborg et al., 2016a).

2.5. Calculations of pools and fluxes

2.5.1. Atmospheric deposition

The low TOC concentrations in rain and snow led us to assume that the only significant input of carbon from the atmosphere at TBL occurs as eolian deposition. The annual eolian deposition on the lake surface was calculated from the TOC data from old snow packs sampled in April. The snow TOC concentration was first corrected for sublimation using data from Johansson et al. (2015a), and the area with snow accumulation was estimated to be 20% of the lake area based on time-lapse photos (Johansson et al., 2015b). Hence, 20% of the winter precipitation directly on to the lake was multiplied by the corrected old snow TOC concentrations. Even though eolian transport is higher during winter (Willemse et al., 2003), eolian deposition also occurs during the four summer months (late May to early September). Therefore, to represent annual eolian deposition, the winter estimate was multiplied by 1.5. For the terrestrial system, we assumed that the carbon input via eolian deposition equals the eolian erosion. The rationale behind this assumption is that if significant accumulation of organic matter did occur in the terrestrial environment it would

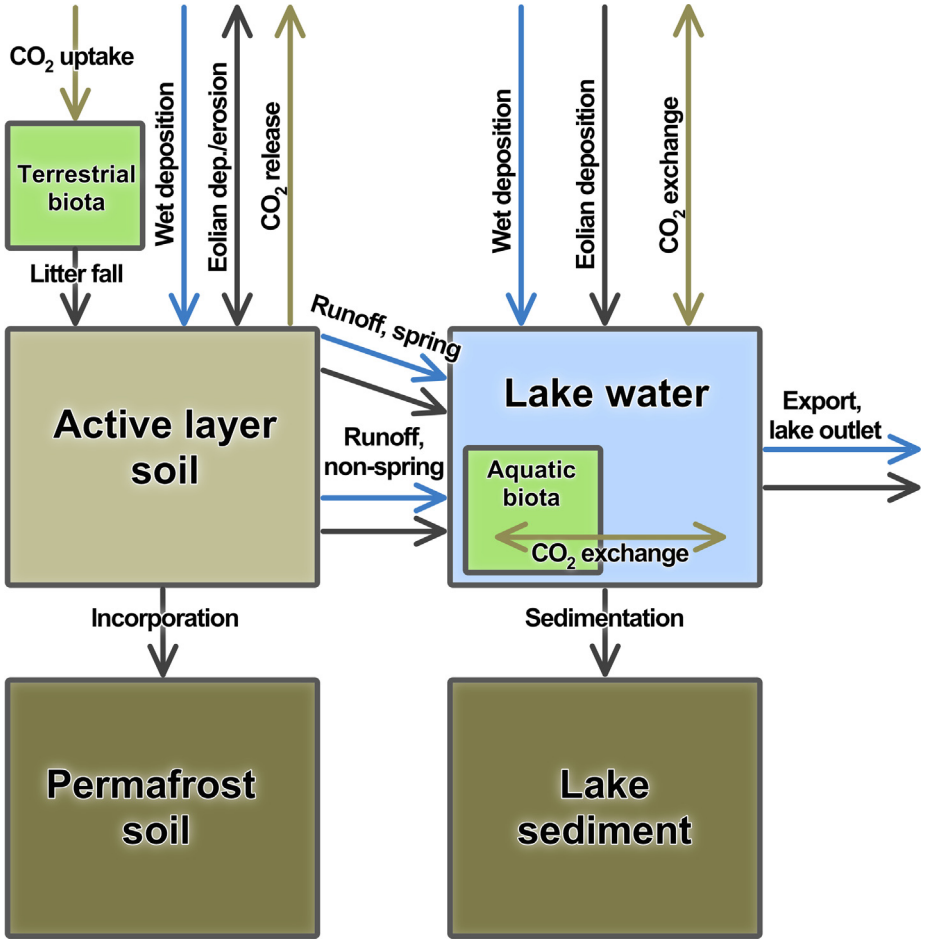

Fig. 3. Conceptual figure describing the different pools and fluxes included in the carbon mass-balance budget. Blue arrows represent dissolved fluxes with water, dark grey arrows represent fluxes of particulate matter and brown represent fluxes of gases.

Table 2
Areal extent of the dominant vegetation types in the TBL catchment together with estimates related to the biomass, net primary production (NPP) and soil organic carbon (SOC) in the active layer and permafrost.

Vegetation type	Area (%)	Biomass[1] (kg C m^{-2})	NPP[1] (g C m^{-2} yr^{-1})	Litter[1] (kg C m^{-2})	Replicates	Active layer SOC (kg C m^{-2})	SOC Replicates	Refractive SOC accumulation rate[2] (g C m^{-2} yr^{-1})	Active layer depth[3] (m)	Permafrost SOC[4] (kg C m^{-2})	Total SOC pool (down to 100 cm) (kg C m^{-2})
Exposed bedrock	7	0	0	0	–	0	–	–	2	0	0
Non-vegetated areas	15	0	0	0	–	7.05	–	–	n.d.	2.85	9.8[5]
Dwarf shrub	14	2.47	147	1.41	5	22.1	4	16.8	0.7	11.7	33.8
Dry grassland	20	0.36	204	1.16	2	10.3	2	8.2	0.8	2.8	13.1
Meadow	38	0.54	217	1.5	5	13.3	2	10.6	0.7	10.1	23.4
Wetland	7	0.91	72	0.82	3	18.5	4	13.8	0.5	17.7	36.2

[1] Includes both above- and below-ground pools/fluxes.
[2] Based on the total SOC and litter pools, and the estimated age (1400 years) of the active layer.
[3] From Petrone et al. (2016).
[4] Permafrost SOC is calculated from the lower limit of the active layer and down to 100 cm soil depth.
[5] Active layer and permafrost SOC pools for non-vegetated areas was not measured, instead the SOC pool below 12 cm soil depth for dry grassland, i.e., the most likely vegetation type to develop wind erosion scars, have been used.

result in visible accumulation of organic material. There is of course some deposition of organic material in depressions and stands with dense vegetation, however this is balanced by the erosion of organic matter in wind exposed locations (Heindel et al., 2017). Here it is important to note that this assumption relates only to organic material and not to the balance between deposition and erosion of mineral material.

2.5.2. Terrestrial pools and fluxes

Living below-ground biomass was estimated by assuming a constant relationship between below-ground and above-ground biomass (2 times for dwarf shrub, and 6 times for meadow and dry grassland; Shaver and Chapin, 1991). For wetlands Shaver and Chapin (1991) found a ratio between below and above-ground biomass of 15:1, however, when using this ratio for TBL

the calculated living below-ground biomass exceeded the total amount of root fragments (living and dead). Therefore, wetlands were assigned the same ratio as meadow and grasslands (6:1). The amount of dead below-ground litter – e.g., dead roots – was calculated as the difference between the measured root content and the estimated below-ground biomass. Above-ground Net Primary Production (NPP) was estimated by multiplying the green biomass (Table 2) – disregarding secondary growth of stems – with different productivity factors. For vascular plants productivity factors of 1, 2 and 3 were used for dwarf shrub, wetland and meadow/dry grassland, respectively. For bryophytes a productivity factor of 0.3 was used for all vegetation types. (Shaver and Chapin, 1991).

Removal of carbon from the catchment by herbivores was based on field estimates of population sizes for muskox and caribou in the Kangerlussuaq area (Cahoon et al., 2012) together with metabolic rates described by an allometric relationship for mammal herbivores (Eq. (2)), which assumes a constant assimilation to consumption efficiency

$$(y = a \times x^b), \quad (2)$$

where y is the field metabolic rate (kJ day^{-1}), x is body mass (g), and a and b are species-specific parameters (Humphreys, 1979; Nagy et al., 1999). This estimate represents the net removal of carbon from the system – i.e., the amount of carbon that either is incorporated as body mass or respired – but excludes the carbon returned to the catchment as excrement.

The soil organic carbon (SOC) pool in the active layer – i.e. the uppermost part of the soil (and/or bedrock) that freezes and thaws every year – was calculated separately for the upper (0–12 cm) and lower (12 cm to permafrost surface) sections of the active layer (active layer depths range from 50 to 80 cm depending on vegetation type; Petrone et al., 2016; Table 2). Everything below the active layer is referred to as the permafrost SOC pool. For the upper section, the SOC calculations were based on measurements of carbon content and bulk density (kg_{DW} m^{-3}) determined from short soil cores (12 cm; sectioned into 3-cm slices). Estimates for the lower section were based on the bulk density from the deepest section of each short core and estimated TOC for deeper sections. TOC concentrations below 12-cm soil depth were estimated by fitting an exponential function to the TOC data from both short and long (40–110 cm) soil cores (Lindborg et al., 2016a). For non-vegetated areas covered by soil, i.e., wind erosion scars, we have used the SOC pool below 12-cm soil depth for dry grassland (i.e., the driest vegetation type that is most prone to develop wind erosion scars).

The permafrost SOC pool was calculated separately for each vegetation type based on the bulk density of the deepest section of the short soil cores and the average TOC concentration of all samples below 30, 9, 30 and 50 cm for dwarf shrub, meadow, dry grassland and wetland vegetation, respectively. Based on the extremely low LOI (<1%) in three till samples we have assumed that the underlying till does not contain significant amounts of carbon, and hence, the permafrost carbon pool is calculated only for the upper layer of eolian silt (i.e., from the permafrost table and down to one-meter soil depth; Table 2; Petrone et al., 2016). As for the active layer SOC-pool we have used the values for dry grassland also for non-vegetated areas covered with silt.

Instead of directly measuring soil respiration, which would require to measure respiration over at least an entire annual cycle, we estimated soil respiration by looking at the long-term net accumulation of carbon in the soil. The SOC accumulation was estimated for each terrestrial vegetation types based on the total carbon pool in the active layer divided by the age of the carbon at the top of the permafrost. The maximum age of the carbon in the active layer was estimated from a soil profile in the wetland vegetation type and was based on the bulk ^{14}C dating (AMS) at the boundary between the active layer and the permafrost at 50 cm soil depth (Lindborg et al., 2016a). Dating soil profiles is difficult and even if there is a general trend with increasing ^{14}C-ages in the soil profiles (Lindborg et al., 2016a,b), the upper 40 cm of the active layer have a modern ^{14}C-signature and the upper 30 cm of the permafrost have a similar age. This suggests an actively cycling system where, e.g., relocation of carbon by roots and cryoturbation affect the ^{14}C signal (Trumbore and Harden, 1997; Becher et al., 2013), which prevents us to establish a reliable age-depth model for the soil profile. For the purpose of this study it is not necessary to know the exact age of a certain soil layer, what we need to know is the maximum and minimum age of the carbon accumulated in the active layer and permafrost, respectively. Therefore, we have – instead of attempting to establish a chronology for the soil profile – simply used the ^{14}C-dates (determined on bulk peat samples) for the samples at the top of the permafrost table and the bottom of the peaty silt to represent the maximum age of the carbon found in the active layer and permafrost, respectively. This allows us to calculate a rough long-term soil respiration estimate by subtracting the SOC accumulation from the estimated total NPP corrected for grazing (i.e., litter production) for each vegetation type (Table 3). The maximum carbon age at the bottom of the peaty silt was 4000 years, which is slightly higher than the maximum age in a long sediment profile from the center of TBL (Rydberg et al., 2016), but lower than the age of the landscape that has been suggested to have been deglaciated some 5000–6800 years ago (van Tatenhove et al., 1996; Levy et al., 2012; Young and Briner, 2015).

2.5.3. Hydrological transport of carbon from the terrestrial to the aquatic system

Johansson et al. (2015a) used a distributed and transient numerical hydrological model to describe variations in water fluxes in the TBL catchment. Based on weather data for a 37-year period this model was used to simulate water-fluxes during hydrological wet, dry and average years. Over the studied period the annual runoff from the terrestrial to the aquatic system varied between 25 and 159 mm per year, with an average of 76 mm per year (normalized over the entire terrestrial catchment area). The modelled runoff during years when the TOC/DOC and DIC were sampled (i.e., 2012, 2013, 2015 and 2017) represented both wet and average year, and TOC/DOC and DIC samples were also collected during both dry (August to September) and wet periods (May) of the year.

The hydrological export of carbon from the terrestrial part of the catchment to the lake was calculated by using the average annual runoff (76 mm or 89,700 m^3) from Johansson et al. (2015a) together with the average TOC/DOC and DIC concentrations in water samples collected in lysimeter installations and from small inlets around the lake (volume × concentration). Our observations suggest that most of the water inflow occurs during a rather limited time period associated with snowmelt, and that transport of water is almost exclusively restricted to the wetland areas in the valleys (Johansson et al., 2015a; Petrone et al., 2016). Observations in May 2016 and May 2017 revealed that, during the snowmelt period, there is an additional area (0.51 km^2) located to the north-east of the TBL-catchment that contributes with runoff to TBL aquatic system. This area is, however, disconnected from the TBL catchment during most of the hydrological year. From the hydrological model we know that about 43% of the runoff occurs during the snow melt period (Johansson et al., 2015a), and hence, we divided the runoff into two periods where one is related to the snow melt period (51,100 m^3) and one represent the remainder of the hydrologically active period (38,600 m^3). For the snowmelt period (spring runoff) the calculations of the runoff include the extended catchment, while for the remainder of the year (non-spring runoff) the calculations are based on the original catchment

Table 3
Carbon pools and fluxes for different components of the TBL catchment.

Pools							
Terrestrial pools	Average (entire terrestrial catchment)[1] kg C m^{-2} or m^{-3}	Average (for relevant part of the terr. catchment)[1] kg C m^{-2} or m^{-3}	Min[2] kg C m^{-2} or m^{-3}	Max[2] kg C m^{-2} or m^{-3}	Total terr. kg C	% total terr.[3]	% of total[3]
Primary producers	6.79E-01	8.66E-01	1.96E-01	3.31E + 00	8.00E + 05	3.1	2.7
Herbivores	8.72E-04	1.22E-03	–	–	1.03E + 03	0.0040	0.0035
SOC active layer (litter incl.)	1.35E + 01	1.89E + 01	7.74E + 00	3.26E + 01	1.59E + 07	62	54
SOC permafrost	7.64E + 00	1.07E + 01	–	–	9.03E + 06	35	30
All terrestrial pools	2.18E + 01	3.05E + 01	–	–	2.57E + 07		87
Aquatic pools	Average (entire lake surface or lake volume)[1] kg C m^{-2} or m^{-3}	Average (for relevant part of the lake surface or lake volume)[1] kg C m^{-2} or m^{-3}	Min[2] kg C m^{-2} or m^{-3}	Max[2] kg C m^{-2} or m^{-3}	Total aqu. kg C	% total aqu.[3]	% of total[3]
Benthic macrophytes	8.78E-02	2.66E-01	7.00E-04	5.53E-01	3.31E + 04	0.85	0.11
Benthic macro fauna	3.24E-04	–	1.70E-05	1.00E-03	1.22E + 02	0.0031	0.0004
Benthic bacteria	8.83E-04	–	2.69E-04	2.09E-03	3.33E + 02	0.0085	0.0011
Phytoplankton[5]	2.89E-05	3.87E-05	1.22E-05	6.20E-05	1.23E + 02	0.0031	0.0004
Zooplankton[5]	4.12E-05	5.51E-05	1.19E-05	7.06E-05	1.75E + 02	0.0045	0.0006
Bacterioplankton[5]	1.43E-05	–	7.23E-06	3.67E-05	6.08E + 01	0.0016	0.0002
Lake water IC[5]	1.69E-02	–	1.42E-02	2.16E-02	7.17E + 04	1.8	0.24
Lake water OC[5]	8.61E-03	–	7.97E-03	9.72E-03	3.66E + 04	0.9	0.12
Sediment	1.00E + 01	1.34E + 01	7.80E+00	1.23E+01	3.77E + 06	96	13
All aquatic pools	1.04E + 01	–	–	–	3.92E + 06		13
Total pool (terr. + aqu.)	1.90E + 01	–	–	–	**2.97E + 07**		–

Fluxes							
Inputs	Compartment	Average (entire compartment)[1] kg C m^{-2} or m^{-3} yr^{-1}	Average (for relevant part of the compartment)[1] kg C m^{-2} or m^{-3} yr^{-1}	Min kg C m^{-2} or m^{-3} yr^{-1}	Max kg C m^{-2} or m^{-3} yr^{-1}	Total flux kg C yr^{-1}	% of total input[4]
Net prim. prod. (NPP)	Terrestrial	1.47E-01	1.88E-01	6.50E-02	3.50E-01	1.74E + 05	99
Atmospheric deposition to lake	Aquatic	1.99E-03	–	–	–	7.50E + 02	0.43
Total Input		1.12E-01				1.75E + 05	–
Internal fluxes	Compartment	Average (entire compartment)[1] kg C m^{-2} or m^{-3} yr^{-1}	Average (for relevant part of the compartment)[1] kg C m^{-2} or m^{-3} yr^{-1}	Min kg C m^{-2} or m^{-3} yr^{-1}	Max kg C m^{-2} or m^{-3} yr^{-1}	Total flux kg C yr^{-1}	% of total input[4]
Prim. prod. to SOC active layer	Terrestial	1.38E-01	1.77E-01	–	–	1.64E + 05	93
Deposition/erosion terrestrial	Terrestrial	–	–	–	–	0.00E + 00	–
DIC from active layer to lake	Terrestial-aquatic	8.27E-04	–	1.44E-04	2.55E-03	9.77E + 02	0.6
TOC from active layer to lake (non-spring runoff)	Terrestial-aquatic	1.36E-03	–	2.76E-04	2.30E-03	1.61E + 03	0.9
TOC from spring flood to lake	Terrestial-aquatic	1.26E-03	–	2.99E-04	3.20E-03	1.49E + 03	0.9
Benthic net primary production	Aquatic	3.89E-03	1.18E-02	0.00E + 00	2.39E-02	1.47E + 03	0.8
Benthic heterotrophic respiration, summer	Aquatic	3.64E-03	–	–	–	1.37E + 03	0.8
Pelagic gross primary production[5]	Aquatic	2.74E-03	3.66E-03	–	–	1.16E + 04	6.7
Pelagic phytoplankton respiration, summer[5]	Aquatic	9.97E-04	1.33E-03	–	–	4.24E + 03	2.4
Pelagic heterotrophic respiration, summer[5]	Aquatic	5.72E-04	–	–	–	2.43E + 03	1.4
Heterotrophic respiration, winter[5]	Aquatic	4.77E-04	–	–	–	2.03E + 03	1.2

(*continued on next page*)

Table 3 (*continued*)

Long-term storage	Compartment	Average (entire compartment)[1]	Average (for relevant part of the compartment)[1]	Min	Max	Total flux	% of total input[4]
		kg C m^{-2} or m^{-3} yr^{-1}	kg C m^{-2} or m^{-3} yr^{-1}	kg C m^{-2} or m^{-3} yr^{-1}	kg C m^{-2} or m^{-3} yr^{-1}	kg C yr^{-1}	
Incorporation in permafrost	Terrestrial	2.94E-03	3.76E-03	0.00E + 00	8.80E-03	3.47E + 03	2.0
Burial in sediment	Aquatic	2.57E-03	3.44E-03	1.40E-03	7.40E-03	9.400E + 02	0.5
Total Storage		2.85E-03				4.44E + 03	2.5
Export	Compartment	Average (entire compartment)[1]	Average (for relevant part of the compartment)[1]	Min	Max	Total flux	% of total input[4]
		kg C m^{-2} or m^{-3} yr^{-1}	kg C m^{-2} or m^{-3} yr^{-1}	kg C m^{-2} or m^{-3} yr^{-1}	kg C m^{-2} or m^{-3} yr^{-1}	kg C yr^{-1}	
From prim. prod. to herbivores	Terrestrial	8.84E-03	1.13E-02	–	–	1.04E + 04	6.0
Heterotrophic soil respiration	Terrestrial	1.30E-01	1.66E-01	1.16E-01	2.75E-01	1.53E + 05	88
Lake water outlet IC[6]	Catchment	5.74E-05	2.37E-04	–	–	8.94E + 01	0.051
Lake water outlet OC[6]	Catchment	2.93E-05	1.21E-04	–	–	4.56E + 01	0.026
Gas flux through lake surface	Aquatic	3.79E-03	–	–	–	1.43E + 03	0.8
Total Export		1.12E-01	–	–	–	1.75E + 05	100.1
Budget imbalance, Terrestial[7]						3.02E + 03	1.7
Budget imbalance, Aquatic[7]						2.32E + 03	48
Budget imbalance, total						5.33E + 03	3.1

[1] Average values are both calculated for the entire terrestrial or aquatic compartments (area or volume), and – where appropriate – for the relevant part of the compartment (e.g., the average carbon pool found in benthic macrophytes are calculated both for the entire lake area and the part of the lake area that is covered with vegetation).
[2] Minimum and maximum values for pools are based on the raw data from the measurements.
[3] Pools are reported both as percent of the terrestrial or aquatic system, and as a percent of the entire catchment pool.
[4] Fluxes are reported as their percent of the total input of carbon.
[5] Averages in kg C m^{-3} or kg C m^{-3} yr^{-1}.
[6] Averages are calculated based on the entire catchment and lake area, respectively.
[7] The percent values are based on the inputs to the terrestrial and aquatic systems, respectively.

area. During an average hydrological year, the extra catchment contributes with 16,700 m^3 of water giving a total spring runoff of 55,200 m^3.

The detailed hydrological modelling was made for the period 2011–2013. It therefore not possible to link most of the TOC/DOC and DIC values in stream and soil water samples, which were collected outside of this time period, to a specific flow of water. Consequently, it was not possible to calculate flow-weighted TOC/DOC and DIC averages. To get an estimate of the theoretical variability in the hydrological input of carbon we calculated a maximum and minimum input using a wet and a dry year. The maximum carbon input was based on the runoff during a wet year (2012; 159 mm or 106,900 and 115,500 m^3 for the non-spring and spring runoff, respectively) together with the average TOC/DOC and DIC plus one standard deviation (33 and 14 mg C L^{-1}, respectively), while the minimum carbon input was based on the runoff during a dry year (2011; 25 mm or 16,800 and 18,200 m^3 for the non-spring and spring runoff, respectively) together with the average TOC/DOC and DIC concentration minus one standard deviations (20 and 5 mg C L^{-1}, respectively).

2.5.4. Aquatic pools and fluxes

The annual net carbon dioxide gas exchange across the lake water surface (F_{CO_2}) was calculated as the average for the period 2011–2013 according to Rocher-Ros et al. (2017; Eq. (3))

$$F_{CO_2} = \varepsilon k_t \left(CO_{2_{water}} - CO_{2_{eqi}} \right), \quad (3)$$

where ε is the chemical enhancement factor (Kuss and Schneider, 2004), k_t is the gas transfer velocity, and $CO_{2_{water}}$ and $CO_{2_{eqi}}$ are the partial presure of CO_2 in the water and in water in equilibrium with the atmosphere, respectively. The k_t for each day during the open-water season was calculated using the Schmidt number for CO_2 (Wanninkhof, 2014), a Schmidt number exponent of −1/2 (Jähne and Haußecker, 1998) and the gas transfer velocity for a gas with a Schmidt number of 600 (k_{600}) based on the lake area and wind speed at 10 m (Vachon and Prairie, 2013). Carbon dioxide partial pressure in the water was calculated based on pH, DIC and water temperature using the fresh water application in the CO2SYS Excel macro (Pierrot et al., 2006). DIC was measured in samples collected in the upper 5-m of the water column on seven occasions in April, June and August during the period 2011–2014. pH at 1-m water depth was measured on eight occasions in April, June and August using an In-Situ Troll 9500 multiparameter instrument (accuracy ± 0.1 pH units). In order to account for the evasion of CO_2 that had accumulated under the ice, the average DIC concentration under the ice in April was used for the first 10 days after ice break up. For July, the average DIC and pH for June and August were used in the calculations, and the August DIC and pH values were used for September. As the relationship between wind speed and k_{600} is site specific we used the range of constants provided by Vachon and Prairie (2013) to also calculate a minimum and maximum CO_2-evasion.

Based on temperature profiles measured in August (n = 5; Lindborg et al., 2016a) the maximum water depth to which the epi- and metalimnion reaches was determined to be about 14 m. The calculations of total phytoplankton, bacterioplankton and zooplankton carbon pools were made separately for the lake volume above and below 14-m water depth. Estimates of the zooplankton carbon pool includes the carbon found in *Branchinecta paludosa*,

which were estimated to have a population density of one individual per cubic meter of water above 14-m water depth. The total macrophyte carbon pool was estimated from the average macrophyte carbon inventory per square meter and the lake-bottom area down to 16-m water depth. Benthic fauna estimates were based on the average carbon inventory per square meter of all samples down to 14-m water depth and the bottom area down to 16-m water. The benthic bacteria carbon pool was estimated separately for shallow (<16 m) and deep (>16 m) areas using the average bacterial carbon inventory per square meter and the lake bottom area for the respective depth interval.

Gross primary production in the pelagic habitat ($GPP_{Pelagic}$) was estimated both from the phytoplankton biomass using carbon-specific respiration rates presented by López-Sandoval et al. (2014), and from the oxygen production (or consumption) in light and dark incubations made in June 2013 (Lindborg et al., 2016a). The hourly $GPP_{Pelagic}$ in five depth intervals (0–1, 1–2, 2–3, 3–5 and 5–10 m) was calculated from the gross oxygen production (i.e., light minus dark incubation) and the volume of each respective depth interval (depths greater than 10 m had negative gross oxygen production and the $GPP_{Pelagic}$ for this part of the lake volume was therefore set to zero). The whole lake $GPP_{Pelagic}$ was then calculated as the sum of all depth intervals and converted to an annual $GPP_{Pelagic}$ by assuming 9 h of production per day during the open-water season from mid-June to mid-September (130 days). Net primary production of the benthic habitat ($NPP_{Benthic}$; including production/respiration of macrophytes, macroalgae, epiphytic algae, phytoplankton and zooplankton) was estimated from the oxygen production (or consumption) during 24 h-incubation in plexiglass chambers placed on the lake bottom (Lindborg et al., 2016a). The $NPP_{Benthic}$-estimates were corrected for benthic bacterial and benthic fauna respiration (calculated based on their respective biomasses, see below for a detailed description), and we applied the June $NPP_{Benthic}$-estimates for the first half of the open-water season and August $NPP_{Benthic}$-estimates for the second half.

Respiration (R) estimates were made separately for the open-water and ice-covered seasons. During the open-water season respiration was estimated for different ecosystem components (e.g., phytoplankton, bacterioplankton, zooplankton, benthic macrofauna and benthic bacteria) based on their respective abundance and conversion factors from the literature. Phytoplankton respiration (R_{Phyto}) was estimated using a relationship established by Tang and Peters (1995; Eq. (4)).

$$R_{Phyto} = 0.0068 * V^{0.88} \quad (4)$$

where R_{Phyto} is the phytoplankton respiration (pL O_2 cell^{-1} h^{-1}) and V is the biovolume (μm^{-3}). For bacterioplankton/benthic bacteria, zooplankton and benthic macrofauna we used carbon specific conversion factors of 0.069, 0.115 and 0.031 g C g^{-1} C day^{-1}, respectively (Kautsky, 1995). As these conversion factors were established at 20 °C, they had to be adjusted for lake water temperature (10 and 5 °C for the epilimnion and hypolimnion, respectively). Respiration during the ice-covered season was estimate based on the oxygen consumption under ice. Oxygen profiles were measured in April 2011, 2013 and 2014, and we assumed that the water column was oxygen saturated in late September when the lake was covered by ice. In April 2011 and 2013 the upper part of the water column was supersaturated with oxygen, which implies that photosynthesis had started already before ice-out. To correct for this oxygen production, we set the maximum oxygen concentration in April to 100% oxygen saturation. All conversions from O_2 consumption/production to CO_2 fixation/release were made using a bacterial respiratory quotient (RQ) of 1.2 (Berggren et al., 2012) and photosynthetic quotient of 1.28 for phytoplankton (Wielgat-Rychert et al., 2017) and 1.2 for benthic macrophytes (Sand-Jensen et al., 2007). We also assumed a molar volume for O_2 of 22.4 l mol^{-1} (at 1 atm).

2.5.5. Sediment accumulation rates

To establish the sediment accumulation over the last 150 years we used either ^{210}Pb activity in bulk sediments (Cores 1, 5, 6, 8, 10 and 13) or ^{14}C determined from macrofossils (cores 2, 7, 12 and 13; Lindborg et al., 2016a). Age-depth models based on ^{210}Pb-data models are known to be sensitive to changes in sediment accumulation rate (Appleby, 2008; Abril and Brunskill, 2014), and a previous study showed that the sediment accumulation rate in the deep basin of TBL has been highly variable (Rydberg et al., 2016). Therefore, we did not develop age-depth models for the sediment cores. Instead we used the ^{210}Pb 99% equilibrium depth (i.e., the depth above which 99% of the unsupported ^{210}Pb-inventory is found) as a way to determine what depth that roughly correspond to 150 years (Oldfield et al., 1995). In the cores where ^{14}C were used, the average sediment accumulation rate (mm yr^{-1}) down to the dated depth was calculated using the calibrated ages. This sediment accumulation rate was then used to calculate the depth that corresponds to 150 years. For the four cores where no dating was made (3, 4, 9 and 11), the sediment depth at 150 years was estimated based on a distinct change in the sediment composition (an increase in carbon), which – based on the dated cores – occurred synchronously across the lake basin about 300 years ago. This depth was then used to estimate the depth that corresponds to 150 years in the same way as for the cores dated with ^{14}C.

The whole basin sediment accumulation rate was then calculated following two different approaches. In the first approach, the lake basin was divided in sub-units based on the bottom type: i) hard rocky erosion bottoms where sediment accumulation was set to zero, ii) areas covered with benthic vegetation (*Chara*, *Nostoc* and bryophytes), and iii) deeper areas with no or limited benthic vegetation. The average carbon accumulation of all sediment cores located within each sub-unit and the areal extent of the sub-unit were used to calculate the whole-lake sediment carbon accumulation. In the second approach, the 13 sediment cores were grouped based on similarities in their composition by using cluster analysis based on the geochemical composition (i.e., concentrations of 25 major and trace elements; Lindborg et al., 2016a). The resulting clusters largely followed water depth, but there were also differences between the northern and southern parts of the basin, presumably because of differences in basin morphology that influence sedimentation and sediment focusing (Blais and Kalff, 1995). Hence, the lake basin was divided into sub-units based on depth zones. For the shallowest zone, which is partly covered with rocky erosion bottoms, the areal extent was reduced to exclude areas with no or very limited sediment accumulation. For both approaches the calculations were made both for the entire lake as one unit and for the northern and southern parts separately in order to capture any potential differences between the northern and southern parts of the lake. To test the sensitivity of the sediment accumulation uncertainties in the estimates of the depth that correspond to 150 years, the carbon accumulation rate was also calculated by reducing or increasing the sections of the sediment used for the calculations by one centimeter (i.e., between 8 and 22% depending on the thickness of the sediment section). Because the sediment burial is based on a 150-year period – and because diagenetic release of carbon to the water column largely is confined to the last 15–20 years (Gälman et al., 2008) – sedimentation is considered as a permanent removal of carbon from the system.

3. Results

3.1. Atmospheric deposition

Because of low DOC concentrations in fresh snow and rain (0.7–0.9 mg L^{-1}; Lindborg et al., 2016b) we assumed that the only significant atmospheric input of organic carbon was as eolian deposition. The TOC concentrations in old snow containing significant amounts particulate organic carbon (POC) from eolian deposition (39–60 mg L^{-1}), which translates to an estimated total input of 750 kg C yr^{-1} to the aquatic system via eolian deposition.

3.2. Terrestrial pools and fluxes

The above- and below-ground carbon biomass for the dwarf shrub, dry grassland, meadow and wetland communities were estimated to be 0.8 and 1.6, 0.05 and 0.3, 0.08 and 0.5, and 0.1 and 0.8 kg C m^{-2}, respectively (Table 2). Together with the areal extent of each vegetation type this gives a standing stock of carbon in terrestrial biomass (above and below ground) for the entire catchment of 801,500 kg C (or on average 870 g C m^{-2}). Using the productivity factors and the biomass values, the average annual net primary production was estimated to 188 g C m^{-2} yr^{-1} based on the vegetated catchment area (Table 3). Large herbivores remove 11 g C m^{-2} yr^{-1} of the annual terrestrial NPP, whereas the remaining 177 g C m^{-2} yr^{-1} is added to the litter layer.

SOC concentrations were in the range of 0.7–36% and 1.1–5.4% C (based on dry weight) in the active layer and permafrost, respectively. All vegetation types had higher carbon concentrations in the uppermost part of the soil profile and displayed steadily decreasing carbon concentrations down towards and into the permafrost (Fig. 4). For all vegetation types where deeper soil samples were available there is a good fit between the extrapolated data and the measured SOC concentrations (Fig. 4). Based on the SOC concentrations, bulk density and thickness of the active layer, we estimated the soil carbon pool in the active layer (down to the permafrost table) to between 0 and 22.1 kg C m^{-2} (Table 2). Recalculated to the entire terrestrial catchment (areas with exposed bed rock included) this gives an average of 13.5 kg C m^{-2}, or a total SOC pool of 15900 tonnes C, for the active layer (Table 3). The permafrost carbon pool was estimated to be between 0 and 17.7 kg C m^{-2} (Table 2), which translates to an average for the entire catchment of 7.6 kg C m^{-2}, or 9000 tonnes C in total (Table 3).

Based on ^{14}C dates from on top of the permafrost table and at the basal layer of the peaty silt in the southern part of the catchment it was estimated that the maximum age of the carbon in the active layer and permafrost was 1400 and 4000 years, respectively (Lindborg et al., 2016a). Using the maximum age in the active layer, i.e., 1400 years and the active layer SOC pool gives an estimated heterotrophic soil respiration of, on average, 166 g C m^{-2} yr^{-1} for the vegetated part of the catchment (Table 3). Similarly, using the estimated maximum and minimum age of the carbon in the permafrost (i.e., 4000 and 1400 years, respectively) gives that – during the history of the TBL of the catchment – on average, 2.9 g C m^{-2} yr^{-1} have been incorporated into the permafrost carbon pool.

3.3. Hydrological transport from the terrestrial to the aquatic system

The ranges of TOC, DOC and DIC in soil and surface water samples were 23–34, 14–36 and 6.2–7.0 mg C L^{-1}, respectively. It is not possible to detect any systematic differences in TOC/DOC between years. Even though the DOC concentrations in samples collected in September of the wet 2012 (22 mg C L^{-1}) is lower than those from June and August of the hydrologically average year of 2013 (32 mg C L^{-1}), they are similar to those from June 2015 (24 mg C L^{-1}), which was a hydrologically average year. For 2013, when DOC and DIC concentrations can be compared between the wetter June and drier August, no difference in either DOC or DIC concentrations can be observed (average DOC and DIC concentrations were 31 and 32 mg C L^{-1} and 6.7 and 6.6 mg C L^{-1} for June and August, respectively). Similarly, there does not appear to be any major differences between the DOC concentrations between soil and surface water (27 and 24 mg C L^{-1} for samples collected in lysimeter installations and small inlets respectively), however, the DIC concentrations were higher in soil water as compared to surface water (12 and 6.6 mg C L^{-1}, respectively).

Based on the runoff and the average concentrations of TOC/DOC and DIC in stream and soil water, the annual input of organic carbon was estimated to 3100 kg OC yr^{-1} (690–7300 kg OC yr^{-1}), whereas the estimate for the transport of inorganic carbon from the catchment to the lake was 980 kg IC yr^{-1} (170–1700 kg IC

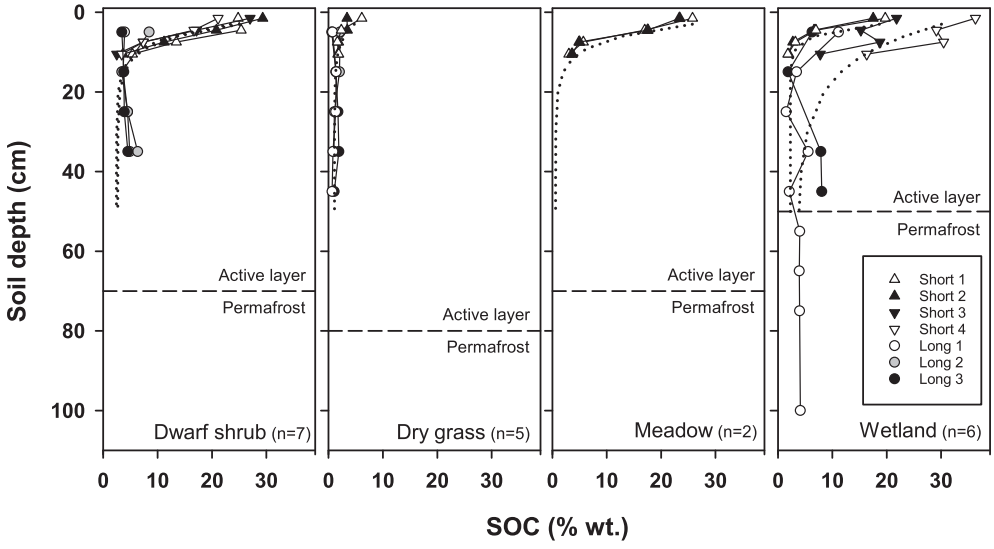

Fig. 4. Soil profiles showing the change in soil organic carbon concentration (SOC) with depth for the different vegetation types (dwarf shrub, dry grassland, meadow and wetland). The dotted lines show the exponential function used to estimate SOC in deeper soil layers, while the horizontal dashed lines represent the depth of the permafrost table in each respective vegetation type. The symbology is the same in all four panels.

yr^{-1}; the ranges represent minimum and maximum inflow based on a dry and wet year and either minus or plus one standard deviation of the DOC/DIC concentrations; Table 3). During an average hydrological year, the input of organic and inorganic carbon related to the snowmelt period were 1600 kg OC yr^{-1} and 510 kg IC yr^{-1}, respectively, whereas the input related to the remainder of the hydrologically active year were 1500 kg OC yr^{-1} and 470 kg IC yr^{-1}, respectively.

3.4. The aquatic system

The ranges for TOC, DOC and DIC in lake water samples were 7.9–10.2, 8.0–9.4 and 14–21 mg C L^{-1}, respectively. Using the lake volume of 4.25 Mm^{-3} this gives an organic carbon pool of, on average, 36600 kg C (33600–43400 kg C) and an inorganic carbon pool of, on average, 71700 kg C (59500–89300 kg C). The carbon biomass in phytoplankton, zooplankton and bacterioplankton was estimated to 12–62, 12–71 and 7.2–37 mg C m^{-3}, respectively. For benthic fauna and benthic bacteria, the carbon biomass was 0.002–1.0 and 0.3–2.1 g C m^{-2}, respectively. Aquatic macrophytes had a carbon biomass of between 0.6 and 680 g C m^{-2}, with low values on wind-exposed shallow areas and the highest values in wind-sheltered shallow areas. This gives that benthic primary producers were by far the largest biotic pool in the lake (33100 kg C or 270 g C m^{-2}), followed by benthic bacteria, zooplankton, phytoplankton, benthic fauna and bacterioplankton (330, 180, 123, 122 and 61 kg C, respectively; Table 3).

Directly following ice-out, when the pH and water temperature were low (7.4 and 5 °C, respectively) and DIC was 15.4–19.5 mg L^{-1}, the modelled lake-water pCO_2 was around 2700 μatm (or 170 μM). In August and September, when the water was warmer (12 °C), pH higher (8.3) and DIC a little lower (14.4–17.7 mg C L^{-1}), pCO_2 was estimated to 330–370 μatm (or 16–22 μM). For the specific dates when DIC was measured during the open water season, modelled pCO_2 was 220, 4761 and 351 μatm for the 19 August 2012, 17 June 2013 and 16 August 2013, respectively. This implies that the lake water in TBL was oversaturated in CO_2 in relation to the atmosphere during the period from ice-out until late July, and close to equilibrium or undersaturated in late summer and autumn. The average k_t values for June, July, August and September were 3.3 (2.3–4.4), 4.6 (3.2–6.0), 3.9 (2.6–5.1) and 3.9 (2.7–5.1) cm h^{-1}, respectively (values in parenthesis represent minimum and maximum k_t as calculated from the range of constants given by Vachon and Prairie, 2013). Together this gives a seasonal trend with CO_2-evasion from ice-out until late July, whereas there is an uptake of CO_2 by the lake water during August and September. Calculated for the entire open-water season there is a net evasion of carbon dioxide from the TBL lake surface to the atmosphere of 1370 (910–1740), 1410 (930–1790) and 1500 (990–1860) kg C yr^{-1} for 2011, 2012 and 2013, respectively (values in parenthesis represent minimum and maximum evasion using different k_t values). This gives an average annual evasion of 3.8 g C m^{-2} yr^{-1} (2.4–4.9 g C m^{-2} yr^{-1}), or 28 mg C m^{-2} day^{-1} (18–38 mg C m^{-2} day^{-1}) if recalculated to an average daily evasion rate per square meter for the open water season.

In the Benthic incubators the average 24-hour oxygen-production were 360 and −12 mg O_2 m^{-2} day^{-1} for June and August, respectively. This translates to a $NPP_{Benthic}$ (after correcting for the benthic bacteria and benthic fauna respiration) of 140 and −59 mg C m^{-2} day^{-1}, and an $NPP_{Benthic}$ for the entire open-water season of 1470 kg C yr^{-1} (or 12 g C m^{-2} yr^{-1} when calculated only for the macrophyte covered part of the lake). The integrated gross oxygen production by phytoplankton down to 10 m in the depth transects was 120 mg O_2 $m^{-2}h^{-1}$ in June and 650 mg O_2 $m^{-2}h^{-1}$ in August, which gives a volume weighted average for the entire lake surface of 89 and 460 mg O_2 $m^{-2}h^{-1}$, respectively. This translates to a daily $GPP_{Pelagic}$ of 240 and 900 mg C m^{-2} day^{-1} for June and August, respectively. The very high $GPP_{Pelagic}$ in August – which is at least an order of magnitude higher than the $GPP_{Pelagic}$ reported for clear-water lakes in the Swedish mountains (Ask et al., 2012) – is largely a consequence of very high oxygen consumption in the dark bottles that results in an unrealistic gross oxygen production. Hence, we have omitted the August measurements and based our annual $GPP_{Pelagic}$-estimate on the June measurements alone. This gives a $GPP_{Pelagic}$ of 11630 kg C yr^{-1} based on the oxygen production in the incubations. This could be compared to the estimates based on the phytoplankton biomass and carbon specific conversion factors, which gave an $GPP_{Pelagic}$ of 7120 kg C yr^{-1} (or 3.7 and 2.2 g C m^{-3} yr^{-1}, respectively, calculated for the lake volume above 14 m). If the respiration of phytoplankton in the epi-/metalimnion (4240 kg C yr^{-1}) is used to recalculate the $GPP_{Pelagic}$ into $NPP_{Pelagic}$ we get an $NPP_{Pelagic}$ of 7390 or 2890 kg C yr^{-1} – or 20 or 7.6 g C m^{-2} yr^{-1} – depending on what $GPP_{Pelagic}$ estimate we use. Together the $NPP_{Benthic}$ and $NPP_{Pelagic}$ gives a total NPP for the aquatic system of 8860 or 4350 kg C yr^{-1}. During the open-water season the heterotrophic respiration in the epilimnion, hypolimnion (including phytoplankton respiration), littoral- and profundal sediments were 1240, 1190, 940 and 430 kg C yr^{-1}, respectively, and from the oxygen consumption under ice it can be determined that an additional 2030 kg C yr^{-1} is respired during winter. This gives a total annual heterotrophic aquatic respiration of 5830 kg C yr^{-1}.

3.5. Lake sediments

Estimated depths that correspond to 150 years were between 3 and 10 cm for the 13 sediment cores. The carbon concentration in sediment samples down to these depths varied from 0.9 to 25% (based on dry weight), and sediment accumulation rates ranged from 0.01 to 0.13 kg dw. m^{-2} yr^{-1}. This gives that the carbon accumulation rate varied between 1.4 and 7.4 g C m^{-2} yr^{-1} across the TBL lake basin. On average, the sediment carbon accumulation rate was 4.1 and 2.9 g C m^{-2} yr^{-1} for the zone with benthic vegetation and deep areas, respectively (approach 1), or 3.9–4.1 and 2.7–2.9 g C m^{-2} yr^{-1} for shallow (<15 m) and deep areas, respectively (approach 2). Recalculated to the entire lake area (including shallow areas without sediment accumulation) this translates to a sediment carbon accumulation rate of 2.5–2.6 g C m^{-2} yr^{-1}, or a total of 940 kg C yr^{-1} for the entire lake basin. If the sediment depth corresponding to 150 years is decreased or increased with one centimetre – to account for uncertainties in the age determinations – the annual whole-lake sediment carbon accumulation was in the range 740–1116 kg C yr^{-1} (or 2.0–3.1 kg C m^{-2} yr^{-1}). If we assume that the time during which sediment accumulation have occurred is 4000 years (based on the basal age of a long sediment profile (Rydberg et al., 2016) and the maximum ^{14}C-age in the terrestrial catchment), this gives a total lake sediment carbon pool of 3770 tonnes (3030–4500 tonnes) or 10 kg C m^{-2} (7.8–12.3 kg C m^{-2}; Table 3).

4. Discussion

4.1. Terrestrial pools and fluxes

Even though the NPP is lower compared to boreal forest ecosystems (Jonsson et al., 2007; Chi et al., 2019) and to a wet site in Siberia (285–476 g C m^{-2} yr^{-1}; Eckhardt et al., 2019), the average NPP for the vegetated parts of the TBL catchment (188 g C m^{-2} yr^{-1}; Table 3) is within the wide range of estimates reported by Wielgolaski et al. (1975) for tundra ecosystems across the Arctic (23–531 g C m^{-2} yr^{-1}). Our estimates of above-ground biomass

(0.05–0.8 kg C m^{-2}) are also similar to those for shrub (0.8 kg m^{-2}), heath (0.2 kg m^{-2}) and wet (0.1 kg m^{-2}) communities from the Toolik-lake area (Shaver and Chapin, 1991). This shows that the TBL catchment and Toolik-lake area are similar in terms of vegetation, and that our use of Shaver and Chapin's (1991) conversion factors for NPP and below-ground biomass is reasonable (although there is still a large potential for errors in the estimates of NPP and below-ground biomass). The estimated living below-ground biomass made up about 78%, 32%, 30% and 76% of the measured total root content (dead and alive) for dwarf shrub, dry grass, meadow and wetland communities, respectively. This indicate that our estimates for below-ground living biomass at least are of the correct magnitude. Under the cold and semi-arid conditions at TBL it is reasonable to expect a higher proportion of dead roots for the dry grass and meadow communities – where decomposition will be limited – as compared to cold and moist or cold and moderately wet conditions (Wielgolaski et al., 1975).

For the TBL area we estimate that ~ 6% or 8.8 g C m^{-2} yr^{-1} of the annual terrestrial NPP is consumed by large herbivores (Table 3). The fact that our estimate is in the lower end of 5–10% range suggested for Arctic regions by Jefferies et al. (1994) and Mulder (1999), could probably be explained by the lack of lemmings at TBL. Several studies in arctic environments have suggested that lemmings and geese are responsible for up to 90% of the grazing effect (Schultz, 1968; Cargill and Jefferies, 1984; Bliss, 1986; Olofsson et al., 2004). Removal of carbon from the terrestrial system is also caused by eolian erosion, which occurs during windy periods. The effects of eolian erosion are clearly visible through the many deflation scars that are present throughout the landscape (Heindel et al., 2017). However, eolian erosion of organic material in the terrestrial system interacts with eolian deposition, and we have assumed a balance between these two processes. This assumption might not be valid for specific locations within the catchment or for the balance between eolian deposition and erosion of mineral material.

Most of the carbon that is added to the soil through litter deposition each year (177 g C m^{-2} yr^{-1}) is respired (166 g C m^{-2} yr^{-1}; Table 3). When compared to other Arctic sites the estimated average long-term respiration rate at TBL is in the upper range of respiration measurements made by Elberling (2007) in East Greenland (Zackenberg) and Svalbard (103, 152 and 176 g C m^{-2} yr^{-1} for moist *Cassiope* heath, dry *Dryas* heath and *Salix* snow beds, respectively). It is also slightly higher than respiration during July to October in the Zackenberg area (148 g C m^{-2} yr^{-1}; Christiansen et al., 2012). This implies that, even though our rough estimate of soil respiration relies heavily on the uncertain estimate of the maximum active-layer carbon-age, it is at least reasonably correct. That we have used an integrative approach to establish the respiration rate – instead of relying on short term direct measurements of soil respiration – also circumvents any issues with inter and intra annual variability in soil respiration, and it accounts also for any losses of carbon through methane emissions, which can be considerable especially in wetter soils (Mastepanov et al., 2013; Geng et al., 2019).

The average active layer SOC pool for the TBL catchment (13.5 kg C m^{-2}) is a bit lower than the average reported for low arctic sites in eastern Siberia (20.3 ± 2.2 kg C m^{-2}), but it is higher than those reported for high arctic sites in the Zackenberg area (8.3 ± 1.3 kg C m^{-2}; Palmtag et al., 2015). In comparison to the range of published active layer SOC pools from Kangerlussuaq region – from 4.8 kg C m^{-2} (Bradley-Cook and Virginia, 2016) to 9.9 kg C m^{-2}, (Henkner et al., 2016) – all four vegetation types at TBL have higher active layer SOC pools (10–22 kg C m^{-2}; Table 2). However, it should be recognized that direct comparisons might be misleading because different studies calculate their active-layer SOC pools down to different soil depths (20 and 30 cm for Bradley-Cook and Virginia (2016) and Henkner et al. (2016), respectively). In studies including soil horizons down to similar depth as in TBL, Jensen et al. (2006) and Elberling et al. (2004) report SOC pools of 2.6–28 and 6.1–22.2 kg C m^{-2} for the Disko bay and Zackenberg areas, respectively (down to 60 and 50 cm, respectively). It is interesting that although the wetland SOC pool from TBL is much lower as compared to boreal peatlands, which are reported to store 72 kg C m^{-2}, the SOC pool in drier, upland vegetation types store similar, or higher, amounts of carbon than upland sites in the boreal landscape in Finland and Sweden (7.2–14 kg; Kauppi et al., 1997; Jonsson et al., 2007). This might be a result of the lower temperature and dry conditions, which limit both degradation and release of organic matter from the soils in the TBL catchment (Laudon et al., 2012).

In contrast to the active layer SOC pool, where most carbon is subjected to various types of degradation, the frozen conditions in the permafrost SOC pool make this pool a more permanent storage than the active layer SOC pool. In the TBL catchment permanently frozen soils store about 35% – or on average 7.6 kg C m^{-2} – of the terrestrial carbon (Table 3). This shows that permafrost soils constitute an important carbon pool in the landscape also under the dry conditions in West Greenland, even though the fraction of SOC found in the permafrost is lower than, e.g., in Siberia where up to half of the total SOC pool can be stored in the permafrost (Siewert et al., 2015). As with the active layer SOC pools it should be recognized that the extent of well-developed wetlands is important for the storage of carbon in permafrost soils on a catchment scale, and even though most of the permafrost carbon is found in the dwarf shrub vegetation type (1900 tonnes C), the wetland areas have the highest carbon pool per unit area (18 kg C m^{-2}). It is also in the wetland areas that the average long-term incorporation of carbon into the permafrost has been highest (6.8 g C m^{-2} yr^{-1}). For the entire catchment, the average long-term incorporation of carbon in the permafrost (2.9 g C m^{-2} yr^{-1}) is of the same magnitude as the average hydrological export of terrestrial carbon to the lake (3.5 g C m^{-2} yr^{-1}). Here it should be recognized that this long-term incorporation into the permafrost was derived from a single ^{14}C-dated bulk sample, and that it reflects the historical incorporation that does not necessarily reflect the present-day conditions.

When looking at the average total SOC pool down to one meter, the average TBL SOC pool (21 kg C m^{-2}) is consistent with the SOC pools (0–100 cm) reported by Hugelius et al. (2013) for upland permafrost soils (i.e., Gelisols of non-histel type) in other arctic regions (13–34 kg C m^{-2} for TBL and, on average, 38 ± 22 kg C m^{-2} for other areas of the arctic). For wetland soil types (Gelisols of Histel-type), wetlands in Alaska, artic Canada and Siberia tend to store more carbon than the wetlands at TBL (36 kg C m^{-2} for TBL, and 71 ± 32 kg C m^{-2} for other parts of the arctic; Hugelius et al., 2013). A likely explanation for this difference could be the drier conditions at TBL, which lead to less developed wetlands. The SOC pools down to 100 cm for the dwarf shrub and wetland communities at TBL (34 and 36 kg C m^{-2}, respectively) are also similar to those found on north-facing slopes at a site located about 20 km south of TBL (36 kg C m^{-2}; Henkner et al., 2016). However, Henkner et al. (2016) report an average SOC pool for all soil types (30 kg C m^{-2}) that is higher than our catchment average of 21 kg m^{-2}. This discrepancy could at least partly be explained by differences in aspect – and associated differences in soil moisture and vegetation – between the studied areas. Most slopes in the TBL catchment, except a small area along the south-eastern shore of the lake, are facing towards the south or south east, and for this type of drier locations Henkner et al. (2016) report a SOC pool (26 kg C m^{-2}) that is more similar to the TBL average.

4.2. Aquatic pools and fluxes

The daily evasion of CO_2 from TBL (28 mg C m^{-2} day^{-1}) is within the wide range of reported values for the boreal region, (Algesten et al., 2005; Lundin et al., 2015). When compared with the values reported by Lundin et al. (2015) for subarctic lakes – on average 16 g C m^{-2} yr^{-1} (1–90 g C m^{-2} yr^{-1}) – the CO_2 evasion in TBL (3.8 g C m^{-2} yr^{-1}) falls in the lower end of the reported range. The annual CO_2-evasion in TBL (Table 3) is also lower when compared to lakes in the Toolik-lake area (Kling et al., 1991). It should be noted that calculations of CO_2-evasion rates based on DIC measurements and carbonate equilibria in general are highly uncertain (Golub et al., 2017), and our calculations are even more uncertain because they are based on a relatively limited number of DIC and pH measurements.

The $GPP_{Pelagic}$ (28 or 17 μg C L^{-1} day^{-1} calculated down to 14-m water depth) in TBL is comparable to the 27 μg C L^{-1} day^{-1} reported for a small lake in arctic Canada (Panzenböck et al., 2000). The open-water season $GPP_{Pelagic}$ (150 or 240 mg C m^{-2} day^{-1} depending on the approach we used) are much higher than those found in Swedish subarctic and boreal lakes (6–46 mg C m^{-2} day^{-1}; Ask et al., 2012). For the higher of our $GPP_{Pelagic}$-estimates – which build on the incubations made in June – it might represent an overestimate of the annual $GPP_{Pelagic}$ because of higher primary productivity in the beginning of the open-water season when limiting nutrients are more abundant (Wetzel, 2001). Also the $NPP_{Benthic}$ in TBL (12 g C m^{-2} yr^{-1} when calculated for only the vegetated area) is higher than the 5.2 g C m^{-2} yr^{-1} reported for a small shallow lake much further north in the Zackenberg area (Riis et al., 2016).

Taken together the pelagic and benthic NPP in TBL (16 and 3.9 g C m^{-2} yr^{-1}, respectively, based on the entire lake area) are almost twice as high as compared to the total NPP reported for lakes in the Toolik-lake area, Alaska (10 g C m^{-2} yr^{-1}: Kling et al., 2000). This difference can likely be explained by the clearer water in TBL (Secchi depth of 15 m) as compared to the Alaskan lakes (Secchi depth of 4 m), which results in much more favourable light conditions in TBL (Karlsson et al., 2009; Mariash et al., 2018). Depending on what estimate for the $GPP_{Pelagic}$ we use (11,630 or 7120 kg C yr^{-1}) the annual balance between aquatic primary production and respiration would give either a positive net ecosystem production (NEP) of 3030 kg C yr^{-1} or a negative NEP of 1470 kg C yr^{-1}. Hence, based on our limited measurements of primary productivity and respiration it is not possible to determine whether the lake is net autotrophic or not (i.e., if GPP > respiration), but even though the aquatic system would be net autotrophic, the loss of carbon through CO_2-evasion from the lake surface shows that the lake is a source of carbon to the atmosphere and that it is dependent on the input of allochthonous carbon from the catchment. That our estimates suggest that TBL is close being in metabolic balance would be consistent with studies in clear-water lakes in the Swedish mountains (Ask et al., 2012).

Our lake sediment carbon accumulation rates are comparable to those reported for other lakes in both the Kangerlussuaq region and for boreal lakes. Anderson et al. (2009) reported values from 3.5 to 11 g C m^{-2} yr^{-1} for eleven lakes from the coast to the ice front, and Sobek et al. (2014) reported carbon accumulation to the sediment in the range of 3.1 to 13 g C m^{-2} yr^{-1} for seven lakes close to Kangerlussuaq. For TBL (or SS903), Sobek et al. (2014) report a carbon accumulation of 5.9 ± 1.1 g C m^{-2} yr^{-1}. Their estimate is within the range of our 13 sediment cores but is higher than our average for the entire lake basin (2.6 g C m^{-2} yr^{-1}). Because Sobek et al. (2014) had the aim to study the organic carbon burial efficiency – and not the sediment carbon accumulation rate for the entire lake basin – no correction for sediment focusing was made. Hence, our value – which take into account the spatial variability in both carbon concentrations and sediment accumulation rates across the lake basin – should be a more robust value for the sediment carbon accumulation rate for the entire TBL lake basin. When compared to other sub-arctic and boreal lakes, the TBL sedimentation rate is comparable to the lower end of the wide ranges reported by Lundin et al. (2015; sub-arctic lakes: 0.6–25 g C m^{-2} yr^{-1} and boreal lakes: 1–90 g C m^{-2} yr^{-1}). Depending on the approach taken in the calculations, the annual incorporation of carbon in the sediment for the entire lake basin was between 930 and 980 kg C yr^{-1} (average 940 kg C yr^{-1}) based on the last 150 years. If we assume a constant sediment composition and a constant sediment accumulation rate for the entire 4000-year during which we know that sediment have accumulated, the total sediment carbon pool would be between 3800 and 4000 tonnes C, or 10.1–10.7 kg C m^{-2}. Considering that the recent carbon accumulation rates are among the lowest in lake's history (Rydberg et al., 2016), and that the landscape is estimated to have been deglaciated some 6800 years ago (Levy et al., 2012) this is most likely an underestimate of the entire sediment carbon pool.

4.3. The carbon budget

The terrestrial primary producer biomass (680 g C m^{-2}) incorporates a net of 150 g C m^{-2} yr^{-1} through primary production. Of this annual terrestrial NPP, 9 g C m^{-2} yr^{-1} are estimated to be removed by herbivores, whereas the remainder is incorporated in the SOC pool as litter. Most of this litter is quickly mineralized and respired back to the atmosphere (130 g C m^{-2} yr^{-1}), but during the course of the catchments history an average of 2.9 g C m^{-2} yr^{-1} have been incorporated into the permafrost pool, whereas 3.5 g C m^{-2} yr^{-1} is exported to the aquatic system as organic carbon and DIC (2.6 g OC m^{-2} yr^{-1} and 0.8 g DIC m^{-2} yr^{-1}; Fig. 4). About half of the hydrological transport is associated with the snow melt period, which shows that it is an important transport route even though it represents much less than half of the unfrozen season (Johansson et al., 2015a). In addition to the input of TOC and DIC with surface and ground water, the lake receives 2.0 g OC m^{-2} yr^{-1} via eolian deposition. Most of the carbon that enters the lake leaves the water column via CO_2-evasion from the lake surface (3.8 g C m^{-2} yr^{-1}) or is buried in the lake sediment (2.6 g C m^{-2} yr^{-1}), while only a small part is exported through the outlet (on average 0.1 g C m^{-2} yr^{-1}; Fig. 5; Table 3)

Overall our mass-balance budget for the entire TBL-catchment is almost in balance, with a positive imbalance of 3% (or 5333 kg C yr^{-1}; Table 3). Similarly, input to the terrestrial system through primary production exceeds the export and long-term storage by only 1.7% (3,460 kg C yr^{-1}; Table 3). This indicates that the assumptions and simplifications made in the model development were reasonable – at least to some extent – and that our empirical data supports our conceptual view of the carbon cycling in the TBL catchment. However, although the terrestrial and whole-catchment carbon budgets are close to being in balance, the aquatic part of the budget is not. Each year 4820 kg C yr^{-1} enters the aquatic system (4100 kg C yr^{-1} through hydrological inputs and 750 kg C yr^{-1} via eolian deposition), while 2540 kg C yr^{-1} leaves the water column (1430 kg C yr^{-1} through CO_2-evasion from the lake surface, 940 kg C yr^{-1} that is buried in sediments and 135 kg C yr^{-1} through the outlet). This gives a positive imbalance for the aquatic system of 2320 kg C yr^{-1} (i.e., 1.5 or 47% of the inputs to the entire catchment and the aquatic systems, respectively: Table 3). This imbalance could be due to both an underestimation of the export or an overestimation of the input, or a combination of both. It could also be a result of the system not being in steady state.

Because of the well constrained hydrologic model and relatively large number of measurements of stream and ground water TOC

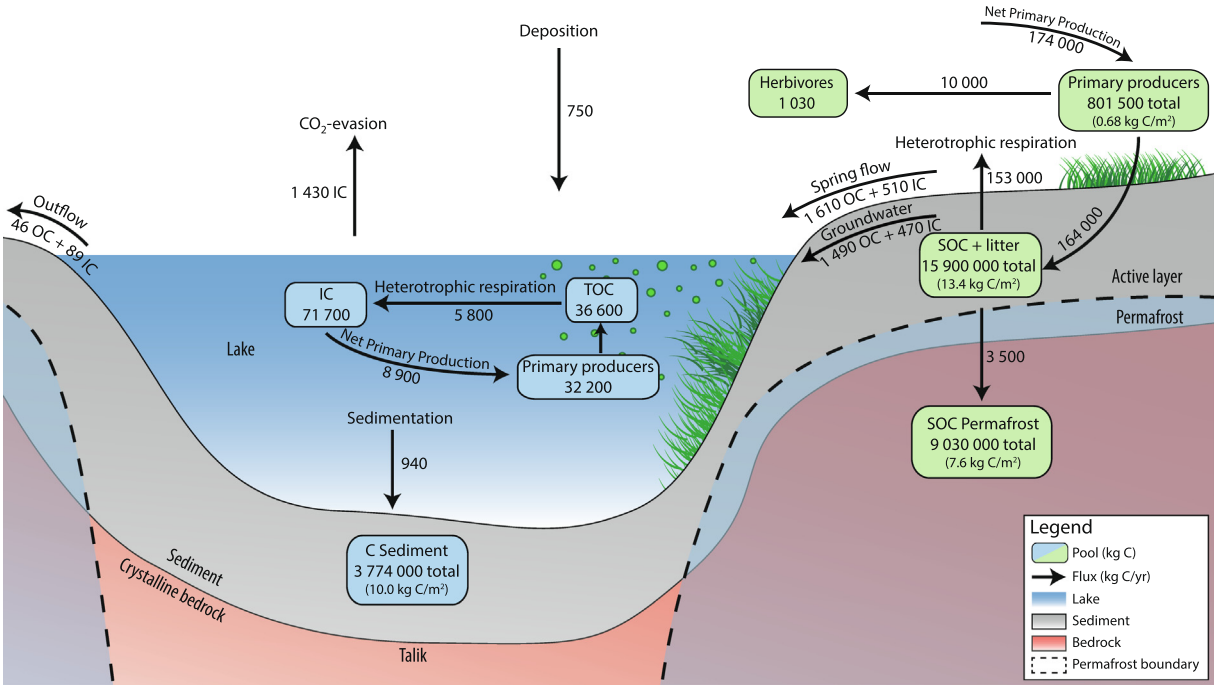

Fig. 5. Conceptual illustration of the carbon landscape ecosystem model for the TBL catchment with pools (kg C) and fluxes (kg C yr^{-1}). Values per unit area are calculated using the area of the entire terrestrial or aquatic system.

and DIC concentrations, we can be relatively confident regarding the average hydrological input of TOC and DIC. However, because our samples are collected during a limited time period it is still possible that inter-annual variability has affected our data. In comparison the estimate of 750 kg C yr^{-1} of eolian deposition is much more uncertain. First, it is based on the accumulation of organic material in old snow packs, which might not be representative. Second, eolian activity is known to be highly variable in time (Rydberg et al., 2016; Willemse et al., 2003; Heindel et al., 2017). Third, the estimate does not consider, e.g., input of leaves during autumn senescence. The input of dead plant material could not only be important for the absolute input of carbon. An input of relatively fresh organic matter would also provide a carbon source that is more easily accessible to the aquatic food web than the heavily degraded humic material that enters the lake through hydrological transport. Over longer time periods it should also be recognized that the quality of the eolian material could vary greatly due to vegetation development and the formation of organic soil horizons (Presthus Heggen et al., 2010). However, even if we reduce the eolian input to zero – which is unrealistic considering the eolian transport that does occur in this landscape (Heindel et al., 2017) – this only affects the aquatic carbon balance marginally. This would suggest that the imbalance is caused by an underestimation of the export of carbon from TBL.

Because it is based on the stable TOC and DIC concentrations of the lake water and the hydrological modelling of the outflow, the export through the outlet is probably the most well constrained flux in the whole budget. Similarly, the sediment burial is relatively well constrained because it builds on sediment cores that capture both spatial and temporal variations. The dating of the sediment profiles introduces some uncertainty, but even if we use the maximum annual sediment burial rate (1116 kg C yr^{-1}) this only accounts for about 8% of the imbalance in the aquatic carbon budget. In contrast the CO_2-evasion from the lake surface is highly uncertain. First, calculations of evasion rates based on wind speed and pCO_2 are known to underestimate the flux when compared to floating chambers (Cole and Caraco, 1998; Macintyre et al., 2010; Vachon et al., 2010; Vachon and Prairie, 2013). Second, our estimate is calculated from modelled pCO_2-values based on a relatively small number of pH and DIC measurement, rather than direct pCO_2-measurements (Golub et al., 2017). Even with these uncertainties it is worth noting, that the ratio between the CO_2 evasion and sediment burial in TBL (1.5) is within the range (2.4 ± 1.7) reported by Lundin et al. (2015) for sub-arctic lakes in northern Sweden. This would suggest that even though the CO_2 evasion is underestimated, the magnitude of the evasion is reasonable. For future work, it should be stressed that – even though the logistical difficulties are large – a much larger effort should be put on better constraining the CO_2-evasion especially directly after ice-out. In addition to the uncertainties related to CO_2-evasion, we also lack data on methane evasion. Methane can be a considerable export pathway for carbon in Arctic lakes (Lundin et al., 2016; Wik et al., 2016). However, this largely applies to small and shallow lakes, whereas the methane evasion from lakes of the same size as TBL only account for a small fraction (<1%) of the carbon export (Holgerson and Raymond, 2016). This, together with the low methane concentrations in the water of lakes close to the ice-margin in West Greenland (including TBL; Northington and Saros, 2016), it is reasonable to assume that methane plays a minor role in the aquatic carbon mass-balance for TBL.

The terrestrial part of the catchment contains about twice as much carbon per unit area as the aquatic system (22 and 10 kg C m^{-2}, respectively). Because of the larger areal extent of the terrestrial part of the TBL catchment, this difference is further enhanced and only about 13% of the total catchment carbon pool is found in the aquatic system. This is much lower than the estimates of Anderson et al. (2009), who concluded that the sediment pool on a landscape scale is about half of the soil pool in the Kangerlussuaq region. This discrepancy might have several causes. First, Anderson et al. (2009) based their calculations for the terrestrial system on a carbon pool of 6.7 kg C m^{-2} (Jensen et al., 2006), which is about one third of the average SOC pool down to 100 cm for the TBL catchment and much lower than SOC pools reported from other places in Greenland (Elberling et al., 2004; Palmtag et al., 2015;

Henkner et al., 2016). Second, even though the carbon accumulation rates in the sediments of TBL are in the lower range of those reported in Anderson et al. (2009), their total lake sediment carbon pools are much higher (42 kg C m^{-2}) than what we find in TBL.

The four times larger sediment pool can partly be explained by differences in the approach used to estimate the sediment carbon pool. Anderson et al. (2009) used one sediment core per lake (not corrected for sediment focusing), while our approach – which relies on 13 spatially distributed sediment cores – captures spatial differences in the sediment carbon accumulation rate across the lake basin. This could have led to an overestimation of the sediment carbon pools in the study reported by Anderson et al. (2009). However, it should also be considered that the sediment record in TBL only spans 4000 years, while many of the lakes used in Anderson et al. (2009) are 7000–9000 years old, which implies that they have had time to accumulate more carbon than TBL. If we instead assume that the TBL has accumulated sediment for 6800 years (Levy et al., 2012), the sediment carbon pool would still only account for about 20% of the catchment carbon pool (6400 tonnes C or 17 kg m^{-2}). In summary, our estimate that about one eighth to one fifth of the total catchment pool is found in the aquatic system is likely more accurate for the younger lakes closer to the ice margin, but it might be an underestimate for older lake catchments further away from the ice sheet.

The export of TOC and DIC from terrestrial soils to the lake is about one third of the carbon export reported for a large boreal catchment in Sweden (8.6 g C m^{-2} yr^{-1}; Jonsson et al., 2007). This difference can at least partly be explained by a combination of low production of TOC and DIC in the soils due to the cold climate and a limited hydrological transport of water due to the dry climate and frozen soils (Laudon et al., 2012). However, the carbon balance in the TBL catchment also differs from the generalized carbon cycling for arctic lakes described by Tranvik et al. (2009). In the Toolik-lake area – which Tranvik et al. (2009) use to describe arctic lakes – the main export route for carbon is downstream transport (78%), whereas for TBL the outlet only accounts for 5% of the export. Instead, most carbon leaves TBL through CO_2-evasion from the lake surface (56%), and sediment burial is higher in relative terms in TBL than in the Toolik-lake area (38% and 2%, respectively). One reason that a higher proportion of the carbon ends up in the sediment in TBL could be the higher relative input of particulate organic carbon (POC) supplied via eolian transport. Because we do not see any significant difference between the lake water TOC and DOC this input of POC likely rapidly passes through the water column and reaches the sediment relatively fast. The input of POC via eolian transport in TBL accounts for 15% of the carbon inputs, whereas the equivalent number for POC in the Toolik-lake area is 3%. These relative numbers, however, do not say anything about the absolute amounts of carbon that are evaded from the lake surface or buried in the sediments. For the export through the lake outlet, there are no major differences between the absolute and relative numbers, and the export in grams per unit area is 17 times higher in the Toolik-lake area than in TBL (1.5 and 0.09 g C m^{-2} yr^{-1}, respectively; Kling et al., 1991). Similarly, the sediment carbon burial per unit area in TBL is twice as high as in the Toolik-lake area (2.6 and 1.3 g C m^{-2} yr^{-1}, respectively; Whalen and Cornwell, 1985). However, although CO_2-evasion in TBL accounts for the majority of the export from the aquatic system the actual CO_2-evasion rates are higher in the Toolik-lake area (24 and 3.6 g C m^{-2} yr^{-1}, respectively; Kling et al., 1991). Hence, regardless of if we use the relative or absolute numbers it is evident that the carbon cycling in the TBL catchment – and presumably also in other dry arctic environments – is different from that of the much wetter periglacial landscapes of Alaska.

Even though the TBL catchment from a geomorphological point of view is stable and not currently affected by proglacial landforming processes, it is unlikely that all catchment processes are in steady state. For example, several West Greenland lakes have been reported to experience decreasing lake water DOC concentrations during the last decades (Saros et al., 2015), and the Kangerlussuaq weather data shows increasing air temperatures over the last 30 years (Cappelen, 2016). Such environmental trends could, of course, have an influence on our mass balance. A decrease in lake water DOC with time would imply that the input of organic carbon from the catchment should be smaller than the evasion of CO_2 from the lake surface due to photo oxidation and microbial respiration in the lake water (Karlsson et al., 2012; Gonsior et al., 2013). Even though our estimates of the CO_2-evasion rate are uncertain, the imbalance in the TBL carbon mass balance would suggest there is no such trend in TBL (CO_2 evasion is smaller than the organic carbon input). A warmer climate would presumably lead to higher rates of primary production, but also a quicker turnover of organic matter in the active layer and potentially to a mobilization of carbon currently locked in the permafrost pool. However, the net result would not only depend on the relative effect on production and degradation of organic matter. It would also make a difference if the higher temperatures result in more complete degradation of the organic matter (i.e., more respiration) or if the production of DOC, and thus the transport to the aquatic system, is favoured. Another important aspect of climate change is whether precipitation will increase or decrease. For the Kangerlussuaq region it is predicted that both temperature and precipitation will increase in the coming 50–100 years (Boberg et al., 2018), but because no predictions regarding changes in evapotranspiration exists it is difficult to assess how this increase in precipitation relates to runoff. An increased annual precipitation could lead to a higher runoff and a shorter water-residence time in the lake and, hence, it might induce changes in the internal carbon cycling in the lake (e.g., photo reduction, carbon sedimentation rates, sediment oxygen exposure and lake water DOC concentrations; Saros et al., 2015; de Wit et al., 2018) and lead to an increased export of carbon through the lake outlet.

4.4. Strengths and limitations

The size of the TBL catchment and the diverse nature of the landscape make it virtually impossible to cover all pools and fluxes with the same temporal and spatial resolutions as when studying only a part of the system or a single process. Instead, the strength of this work is that it integrates the entire catchment and benefits significantly from the extensive work on constraining the hydrology, meteorology and catchment morphology of the catchment (Johansson et al., 2015a,b; Petrone et al., 2016). This gives us a solid basis for our carbon mass-balance, especially when looking at the carbon pools.

Even with the well constrained background conditions there are many uncertainties in our data. Partly this relates to the fact that our estimates rely on spot measurements rather than continuous measurements, which leaves gaps in our data series. The most prominent gaps in our data series relate to the CO_2-evasion, where more frequent measurements of pH, DIC or dissolved CO_2 in the lake water would significantly improve the reliability of our estimates. Because CO_2 might build up under ice it is particularly problematic that we lack measurements from the period directly after ice-out. There are also gaps in the TOC and DIC measurements in the runoff from the terrestrial system. This prevents us from making reliable intra annual comparisons and to calculate flow weighted averages, but because we do have data from both high, medium and low flow situations the data should give a good representation of the average input of TOC and DIC to the aquatic system. For some fluxes (soil respiration, incorporation into permafrost soils and sediment burial) we have used integrative approaches looking at the long-term net effect of these processes

rather than trying to up-scale direct measurements. However, this introduces other uncertainties related age estimates needed for these calculations (e.g., issues with dating).

Further investigations could improve this carbon mass-balance, especially when it comes to better constraining and reducing the uncertainties associated to some of the fluxes. As mentioned, one of the major uncertainties is the CO_2-evasion from the lake water surface, which could be much better constrained. Similarly, additional analyses of ^{14}C in the active layer and permafrost would give a much better constraint on the carbon incorporation in soils, and even though eolian erosion and deposition are difficult to measure accurately such measurements should be given more attention in future studies.

4.5. Conclusion

Our carbon-mass balance for the TBL catchment highlights four key points. First, most of the carbon in the TBL-catchment (87% or 31 kg m^{-2}) is found in the terrestrial system, with the soil organic carbon-pools accounting for 54% (or 13 kg m^{-2}) and 30% (or 7.6 kg m^{-2}) for the active layer and permafrost, respectively. That 30% of the catchment carbon (or 35% of the terrestrial carbon) is stored in permafrost soils shows that permafrost soils are an important carbon accumulation feature in this landscape. Second, the long-term incorporation of carbon in permafrost soils and lake sediment is relatively similar per unit area (2.9 and 2.6 g C m^{-2} yr^{-1}, respectively), but the much larger terrestrial area translates to a three times higher carbon incorporation in the terrestrial system as compared to the aquatic system (3500 vs. 940 kg C yr^{-1}). Third, the hydrologic transport of carbon from the terrestrial system to the lake (3.5 g C m^{-2} yr^{-1}) is lower than in boreal systems (6–12 g C m^{-2} yr^{-1}; Jonsson et al., 2007), but it is still the most important input of carbon to the aquatic system and delivers more than five times as much carbon as eolian processes (4100 and 750 kg C yr^{-1}, respectively). Fourth, the net evasion of CO_2 from the lake surface indicates that the lake is a source of carbon to the atmosphere.

Regardless of the uncertainties this carbon mass-balance budget does show that some aspects of the carbon cycling in this dry and cold region is different from those described for wetter parts of the Arctic. This shows that the Arctic is heterogeneous, and that any single site – including the TBL catchment – provides just one piece of the puzzle depicting the Arctic carbon cycling. By combining the results from this piece with those from other typical and atypical sites will then allow us to obtain a reliable carbon mass-balance budget for the entire Arctic region.

CRediT authorship contribution statement

Lindborg Tobias: Conceptualization, Investigation, Writing - original draft, Visualization, Project administration. **Rydberg Johan:** Investigation, Writing - original draft, Visualization. **Andersson Eva:** Investigation, Writing - original draft. **Löfgren Anders:** Investigation, Writing - original draft. **Lindborg Emma:** Conceptualization, Investigation, Methodology, Writing - review & editing, Project administration. **Saetre Peter:** Investigation, Writing - original draft. **Sohlenius Gustav:** Investigation. **Berglund Sten:** Investigation, Writing - review & editing. **Kautsky Ulrik:** Conceptualization, Writing - review & editing, Funding acquisition. **Laudon Hjalmar:** Conceptualization, Investigation, Writing - review & editing, Supervision.

Acknowledgements

This work was conducted as a part of the Greenland Analogue Surface Project (GRASP) funded by the Swedish Nuclear Fuel and Waste Management Company (SKB). The authors would like to thank the Greenland Analogue Project (GAP) and Kangerlussuaq International Science Support (KISS) for providing logistical support throughout the years. We thank Johannes Petrone for help with conceptual illustrations. The authors would also like to thank Dr. Mike Thorne for valuable comments on earlier versions of this paper. Finally, we thank four anonymous reviewers for helping us to significantly improve our work.

Appendix A. Supplementary data

Supplementary data to this article can be found online at https://doi.org/10.1016/j.scitotenv.2019.134561.

References

Abril, J.-M., Brunskill, G., 2014. Evidence that excess 210Pb flux varies with sediment accumulation rate and implications for dating recent sediments. J. Paleolimnol. 2014, 1–17.
Algesten, G., Sobek, S., Bergström, A.-K., Jonsson, A., Tranvik, L.J., Jansson, M., 2005. Contribution of sediment respiration to summer CO_2 emission from low productive boreal and subarctic lakes. Microb. Ecol. 50, 529–535.
Andersson, E., Sobek, S., 2006. Comparison of a mass balance and an ecosystem approach when evaluating the carbon cycling in a lake ecosystem. Ambio 35, 476–483.
Anderson, N.J., D'Andrea, W., Fritz, S.C., 2009. Holocene carbon burial by lakes in SW Greenland. Glob. Change Biol. 15, 2590–2598.
Appleby, P.G., 2008. Three decades of dating recent sediments by fallout radionuclides: a review. Holocene 18 (1), 83–93.
Ask, J., Karlsson, J., Jansson, M., 2012. Net ecosystem production in clear-water and brown-water lakes. Global Biogeochem. Cycles 26, GB1017.
Becher, M., Olid, C., Klaminder, J., 2013. Buried soil organic inclusions in non-sorted circles fields in northern Sweden: age and paleoclimatic context. J. Geophys. Res.-Biogeosci. 118, 104–111.
Berggren, M., Lapierre, J.F., del Giorgio, P.A., 2012. Magnitude and regulation of bacterioplankton respiratory quotient across freshwater environmental gradients. ISME J. 6, 984–993.
Bliss, L.C., 1986. Arctic ecosystems: their structure, function and herbivore carrying capacity, in Gudmundsson (Ed.), Grazing research at northern latitudes. Plenum, pp. 5–26.
Blais M., J., Kalff, J., 1995. The Influence of Lake Morphometry on Sediment Focusing. Limnology and Oceanorgaphy 40 (3), 582–588.
Boberg, F., Langen, P.L., Mottram, R.H., Christensen, J.H., Olesen, M., 2018. 21st-century climate change around Kangerlussuaq, west Greenland: from the ice sheet to the shores of Davis Strait. Arct. Antarct. Alp. Res. 50, S100006. https://doi.org/10.1080/15230430.2017.1420862.
Bradley-Cook, J.I., Virginia, R.A., 2016. Soil carbon storage, respiration potential, and organic matter quality across an age and climate gradient in southwestern Greenland. Polar Biol. 39, 1283–1295.
Bronk Ramsey, C., 2009. BAYESIAN ANALYSIS OF RADIOCARBON DATES. RAdiocarbon 51 (1), 337–360.
Cahoon, S.M.P., Sullivan, P.F., Post, E., Welker, M.W., 2012. Large herbivores limit CO_2 uptake and supress carbon cycle responses to warming in West Greenland. Glob. Change Biol. 18, 469–479.
Cappelen, J. (Ed.), 2016. Weather observations from Greenland 1958–2015, Observation data with description: DMI Report 16–08. Danish Meteorological Institute, Copenhagen, Denmark.
Cargill, S.M., Jefferies, R.L., 1984. The effects of grazing by Lesser Snow Geese on the vegetation of a subarctic salt marsh. J. Appl. Ecol. 21, 669–686.
Chi, J.S., Nilsson, M.B., Kljun, N., Wallerman, J., Fransson, J.E.S., Laudon, H., et al., 2019. The carbon balance of a managed boreal landscape measured from a tall tower in northern Sweden. Agric. For. Meteorol. 274, 29–41.
Christiansen, C.T., Svendsen, S.H., Schmidt, N.M., Michelsen, A., 2012. High arctic heath soil respiration and biogeochemical dynamics during summer and autumn freeze-in - effects of long-term enhanced water and nutrient supply. Glob. Change Biol. 18 (10), 3224–3236.
Cole, J.J., Caraco, N.F., 1998. Atmospheric exchange of carbon dioxide in a low-wind oligotrophic lake measured by the addition of SF_6. Limnol. Oceanogr. 43, 647–656.
de Wit, H.A., Couture, R.M., Jackson-Blake, L., Futter, M.N., Valinia, S., Austnes, K., Guerrero, J.-L., Lin, Y., 2018. Pipes or chimneys? For carbon cycling in small boreal lakes, precipitation matters most. Limnol. Oceanogr. Lett. 3, 275–284.
Eckhardt, T., Knoblauch, C., Kutzbach, L., Holl, D., Simpson, G., Abakumov, E., et al., 2019. Partitioning net ecosystem exchange of CO2 on the pedon scale in the Lena River Delta, Siberia. *Biogeosciences* 16, 1543–1562.
Elberling, B., 2007. Annual soil CO_2 effluxes in the High Arctic: the role of snow thickness and vegetation type. Soil Biol. Biochem. 39, 646–654.
Elberling, B., Jakobsen, B.H., Berg, P., Sondergaard, J., Sigsgaard, C., 2004. Influence of vegetation, temperature, and water content on soil carbon distribution and mineralization in four high Arctic soils. Arct. Antarct. Alp. Res. 36, 528–538.

Engels, S., Helmens, K., 2010. Holocene environmental changes and climate development in Greenland.: SKB R-10-65, Swedish Nuclear Fuel and Waste Management Co. Stockholm, Sweden.
Frey, K.E., Smith, L.C., 2005. Amplified carbon release from vast West Siberian peatlands by 2100. Geophys. Res. Lett. 32 (9), L09401.
Geng, M.S., Christensen, J.H., Christensen, T.R., 2019. Potential future methane emission hot spots in Greenland. Environ. Res. Lett. 14, 035001.
Golub, M., Desai, A.R., McKinley, G.A., Remucal, C.K., Stanley, E.H., 2017. Large uncertainty in estimating pCO2 from carbonate equilibria in lakes. J. Geophys. Res. Biogeosci. 122 (11), 2909–2924.
Gonsior, M., Schmitt-Kopplin, P., Bastviken, D., 2013. Depth-dependent molecular composition and photo-reactivity of dissolved organic matter in a boreal lake under winter and summer conditions. Biogeosciences 10 (11), 6945–6956.
Gälman, V., Rydberg, J., Sjöstedt de-Luna, S., Bindler, R., Renberg, I., 2008. Carbon and nitrogen loss rates during ageing of lake sediment: Changes over 27 years studied in a varved lake sediment. Limnol. Oceanogr. 53, 1076–1082.
Hanna, E., Mernild H., S., Cappelen, J., Steffen, K., 2012. Recent warming in Greenland in a long-term instrumental (1881-2012) climatic context: I. Evaluation of surface air temperature records. Environmental Research Letters 7, (4) 045404.
Hanson, P.C., Pace, M.L., Carpenter, S.R., Cole, J.J., Stanley, E.H., 2015. Integrating landscape carbon cycling: research needs for resolving organic carbon budgets of lakes. Ecosystems 18, 363–375. https://doi.org/10.1007/s10021-014-9826-9.
Harper, J., Hubbard, A., Ruskeeniemi, T., Claesson Liljedahl, L., Lehtinen, A., Booth, A., Brinkerhoff, D., Drake, H., Dow, C., Doyle, S., Engström, J., Fitspatrik, A., Frape, S., Henkemans, E., Humphrey, N., Johnsson, J., Jones, G., Joughin, I., Klint, K.E., Kukkonen, I., Kulessa, B., Londowski, C., Lindbäck, K., Makahnouk, M., Meierbachtol, T., Pere, T., Pedersen, K., Pettersson, R., Pimentel, S., Quincey, D., Tullborg, E.-L., van As, D., 2011. In: *The Greenland Analogue Project Yearly Report 2010*. Swedish Nuclear Fuel and Waste Management Co., SKB, Stockholm, Sweden, p. R-11-23..
Heindel, R.C., Culler, L.E., Virginia, R.A., 2017. Rates and processes of aeolian soil erosion in West Greenland. The Holocene 27, 1–10.
Henkner, J., Scholten, T., Kühn, P., 2016. Soil organic carbon stocks in permafrost-affected soils in West Greenland. Geoderma 282, 147–159.
Hobbie, S.E., Schimel, J.P., Trumbore, S.E., 2000. Controls over carbon storage and turnover in high-latitude soils. Glob. Change Biol. 6, 196–210.
Holgerson, M.A., Raymond, P.A., 2016. Large contribution to inland water CO2 and CH4 emissions from very small ponds. Nat. Geosci. 9, 222–226.
Hollesen, J., Elberling, B., Jansson, P.E., 2011. Future active layer dynamics and carbon dioxide production from thawing permafrost layers in Northeast Greenland. Glob. Change Biol. 17 (2), 911–926.
Hua, Q., Barbetti, M., Rakowski Z., A., 2013. Atmospheric radiocarbon for the period 1950-2010. Radiocarbon 55 (4), 2059–2072.
Hugelius, G., Bockheim, J., Camill, P., Elberling, B., Grosse, G., Harden, J., et al., 2013. A new data set for estimating organic carbon storage to 3 m depth in soils of the northern circumpolar permafrost region. Earth Syst. Sci. Data 5, 393–402. https://doi.org/10.5194/essd-5-393-2013.
Humphreys, W.F., 1979. Production and respiration in animal populations. J. Anim. Ecol. 48, 427–453.
IPCC, 2013. Climate change 2013: the physical science basis. In: Stocker, T.F., Qin, D., Plattner, G.-.K., Tignor, M., Allen, S.K., Boschung, J., Nauels, A., Xia, Y., Bex, V., Midgley, P.M. (Eds.), Contribution of Working Group I to the Fifth Assessment Report of the Intergovernmental Panel on Climate Change. Cambridge University Press, Cambridge, United Kingdom and New York, NY, USA.
Jefferies, R.L., Klein, D.R., Shaver, G.R., 1994. Vertebrate herbivores and northern plant communities: reciprocal influences and responses. Oikos 71, 193–206.
Jensen, L.A., Schmidt, L.B., Hollesen, J., Elberling, B., 2006. Accumulation of soil organic carbon linked to Holocene sea level changes in west Greenland. Arct. Antarct. Alp. Res. 38, 378–383.
Johansson, E., 2019. Extension of the dataset "Hydrological and meteorological investigations in a periglacial lake catchment near Kangerlussuaq, West Greenland". PANGAEA. https://doi.org/10.1594/PANGAEA.900595.
Johansson, E., Gustafsson, L.-G., Berglund, S., Lindborg, T., Selroos, J.-O., Claesson Liljedahl, L., Destouni, G., 2015a. Data evaluation and numerical modeling of hydrological interactions between active layer, lake and talik in a permafrost catchment, Western Greenland. J. Hydrol. 527, 688–703.
Johansson, E., Berglund, S., Lindborg, T., Petrone, J., van As, D., Gustafsson, L.-G., Näslund, J.-O., Laudon, H., 2015b. Hydrological and meteorological investigations in a periglacial lake catchment near Kangerlussuaq, west Greenland – presentation of a new multi-parameter data set. Earth Syst. Sci. Data 7, 93–108. https://doi.org/10.5194/essd-7-93-2015.
Johansson, J.-Å., Olofsson, H., Ramberg, L., 1976. Studier av zooplanktons konsumtion i Botjärn. (Studies regarding zooplankton consumption in the lake Botjärn). Klotenprojektets rapport nr. 5. Department of Limnology, Uppsala University, p. 22.
Jonsson, A., Algesten, G., Bergstrom, A.K., Bishop, K., Sobek, S., Tranvik, L.J., Jansson, M., 2007. Integrating aquatic carbon fluxes in a boreal catchment carbon budget. J. Hydrol. 334, 141–150.
Jähne, B., Haußecker, H., 1998. Air-water gas exchange. Annu. Rev. Fluid Mech. 30 (1), 443–468.
Karlsson, J., Bystrom, P., Ask, J., Ask, P., Persson, L., Jansson, M., 2009. Light limitation of nutrient-poor lake ecosystems. Nature 460 (7254), 506–509.
Karlsson, J., Berggren, M., Ask, J., Bystrom, P., Jonsson, A., Laudon, H., Jansson, M., 2012. Terrestrial organic matter support of lake food webs: evidence from lake metabolism and stable hydrogen isotopes of consumers. Limnol. Oceanogr. 57 (4), 1042–1048.
Kauppi, P.E., Posch, M., Hänninen, P., Henttonen, H.M., Ihalainen, A., Lappalainen, E., Starr, M., Tamminen, P., 1997. Carbon reservoirs in peatlands and forests in the boreal regions of Finland. Silva Fennica 31, 13–25.
Kautsky, U., 1995. *Ecosystem Processes in Coastal Areas of the Baltic Sea*. Ph.D. thesis. Department of Zoology, Stockholm University, Sweden.
Kemp, P.F., Cole, J.J., Sherr, B.F., Sherr, E.B., 1993. Handbook of Methods in Aquatic Microbial Ecology. CRC Press. ISBN 9780873715645.
Kling, G.W., Kipphut, G.W., Miller, M.C., 1991. Arctic lakes and streams as gas conduits to the atmosphere – Implications for tundra carbon budgets. Science 251 (4991), 298–301.
Kling, G.W., Kipphut, G.W., Miller, M.M., O'Brien, W.J., 2000. Integration of lakes and streams in a landscape perspective: the importance of material processing on spatial patterns and temporal coherence. Freshw. Biol. 43 (3), 477–497.
Koenigk, T., Brodeau, L., Graversen G., R., Karlsson, J., Svensson, G., Tjernström, M., Willén, U., Wyser, K., 2013. Arctic climate change in 21st century CMIP5 simulations with EC-Earth. Climate dynamics 40 (11), 2719–2743.
Kuss, J., Schneider, B., 2004. Chemical enhancement of the CO_2 gas exchange at a smooth seawater surface. Mar. Chem. 91 (1), 165–174.
Lapierre, J.-F., del Giorgio, P.A., 2012. Geographical and environmental drivers of regional differences in the lake pCO(2) versus DOC relationship across northern landscapes. J. Geophys. Res. 117, G03015. https://doi.org/10.1029/2012JG001945.
Laudon, H., Buttle, J., Carey, S.K., McDonnell, J., McGuire, K., Seibert, J., Shanley, J., Soulsby, C., Tetzlaff, D., 2012. Cross-regional prediction of long-term trajectory of stream water DOC response to climate change. Geophys. Res. Lett. 39, L18404.
Lehmann-Konera, S., Kociuba, W., Chmiel, S., Franczak, L., Polkowska, Z., 2019. Concentrations and loads of DOC, phenols and aldehydes in a proglacial arctic river in relation to hydro-meteorological conditions. A case study from the southern margin of the Bellsund Fjord-SW Spitsbergen. Catena 174, 117–129.
Levy, L.B., Kelly, M.A., Howley, J.A., Virginia, R.A., 2012. Age of the Orkendalen moraines, Kangerlussuaq, Greenland: constraints on the extent of the southwestern margin of the Greenland Ice Sheet during the Holocene. Quat. Sci. Rev. 52, 1–5.
Lindborg, T., Rydberg, J., Tröjbom, M., Berglund, S., Johansson, E., Löfgren, A., Saetre, P., Nordén, S., Sohlenius, G., Andersson, E., Petrone, J., Borgiel, M., Kautsky, U., Laudon, H., 2016a. Biogeochemical data from terrestrial and aquatic ecosystems in a periglacial catchment, West Greenland. *Earth Syst. Sci. Data* 8, 439–459. https://doi.org/10.5194/essd-8-439-2016.
Lindborg, T., Rydberg, J., Tröjbom, M., Berglund, S., Johansson, E., Löfgren, A., Saetre, P., Nordén, S., Sohlenius, G., Andersson, E., Petrone, J., Borgiel, M., Kautsky, U., Laudon, H., 2016b. Biogeochemical data from terrestrial and aquatic ecosystems in a periglacial catchment, West Greenland. doi:10.1594/PANGAEA.860961.
Loferer-Krossbacher, M., Klima, J., Psenner, R., 1998. Determination of bacterial cell dry mass by transmission electron microscopy and densitometric image analysis. Appl. Environ. Microbiol. 64 (2), 688–694.
Lopez-Sandoval, D.C., Rodriguez-Ramos, T., Cermeno, P., Sobrino, C., Maranon, E., 2014. Photosynthesis and respiration in marine phytoplankton: relationship with cell size, taxonomic affiliation, and growth phase. J. Exp. Mar. Biol. Ecol. 457, 151–159.
Lundin, E.J., Klaminder, J., Bastviken, D., Olid, C., Hansson, S.V., Karlsson, J., 2015. Large difference in carbon emission-burial balances between boreal and arctic lakes. Sci. Rep. 5, 14248. https://doi.org/10.1038/srep14248.
Lundin, E.J., Klaminder, J., Giesler, R., Persson, A., Olefeldt, D., Heliasz, M., Christensen, T.R., Karlsson, J., 2016. Is the subarctic landscape still a carbon sink? Evidence from a detailed catchment balance. *Geophys. Res. Lett.* 43, 1988–1995.
Löfgren, A., Miliander, S., Truvé, J., Lindborg, T., 2006. Carbon budgets for catchments across a managed landscape mosaic in south-east Sweden: Contributing to the safety assessment of a nuclear waste repository. Ambio 35, 459–468.
Löfgren A. (Ed.), 2010. The terrestrial ecosystems at Forsmark and Laxemar-Simpevarp. SR-Site Biosphere. SKB TR-10-01, Svensk Kärnbränslehantering AB, Stockholm. Sweden.
Macintyre, S., Jonsson, A., Jansson, M., Aberg, J., Turney, D., Miller, S.D., 2010. Buoyancy flux, turbulence, and the gas transfer coefficient in a stratified lake. Geophys. Res. Lett. 37, L24604.
Mariash, H.L., Cazzanelli, M., Rautio, M., Hamerlik, L., Wooller, M.J., Christoffersen, K. S., 2018. Changes in food web dynamics of low Arctic ponds with varying content of dissolved organic carbon. Arct. Antarct. Alp. Res. 50, (1) e1414472.
Mastepanov, M., Sigsgaard, C., Mastepanov, M., Strom, L., Tamstorf, M.P., Lund, M., Christensen, T.R., 2013. Revisiting factors controlling methane emissions from high-Arctic tundra. Biogeosciences 10 (7), 5139–5158.
Matzner, E., Borken, W., 2008. Do freeze-thaw events enhance C and N losses from soils of different ecosystems? A review. Eur. J. Soil Sci. 59, 274–284.
McGuire, A.D., Anderson, L.G., Christensen, T.R., Dallimore, S., Guo, L., Hayes, D.J., Heimann, M., Lorenson, T.D., Macdonald, R.W., Roulet, N., 2009. Sensitivity of the carbon cycle in the Arctic to climate change. Ecol. Monogr. 79, 523–555. https://doi.org/10.1890/08-2025.1.
Metcalfe, D.B., Hermans, T.D.G., Ahlstrand, J., Becker, M., Berggren, M., Bjork, R.G., et al., 2018. Patchy field sampling biases understanding of climate change impacts across the Arctic. Nat. Ecol. Evol. 2, 1443–1448.

Mikan, C.J., Schimel, J.P., Doyle, A.P., 2002. Temperature controls of microbial respiration in arctic tundra soils above and below freezing. Soil Biol. Biochem. 34, 1785–1795.
Mulder, C.P.H., 1999. Vertebrate herbivores and plants in the arctic and subarctic: effects on individuals, populations, communities and ecosystems. Perspect. Plant Ecol. Evol. Systematics 2, 29–55.
Nagy, K.A., Girard, I.A., Brown, T.K., 1999. Energetics of free-ranging mammals, reptiles and birds. Annu. Rev. Nutr. 19, 247–277.
Northington, R.M., Saros, J.E., 2016. Factors controlling methane in Arctic Lakes of Southwest Greenland. PLoS ONE 11, (7) e0159642.
Oldfield, F., Richardson, N., Appleby G., P., 1995. Radiometric dating (^{210}Pb, ^{137}Cs, ^{241}Am) of recent ombrotrophic peat accumulation and evidence for changes in mass balance. Holocene 5 (2), 141–148.
Olofsson, J., Stark, S., Oksanen, L., 2004. Reindeer influence on ecosystem processes in the tundra. Oikos 105, 386–396.
Olrik, K., Blomqvist, P., Brettum, P., Cronberg, G., Eloranta, P., 1998. Methods for quantitative assessment of phytoplankton in freshwaters, part I. Report from Naturvårdsverket, Stockholm, Sweden, no. 4860. 86 pp.
Palmtag, J., Hugelius, G., Lashchinskiy, N., Tamstorf, M.P., Richter, A., Elberling, B., Kuhry, P., 2015. Storage, landscape distribution, and burial history of soil organic matter in contrasting areas of continuous permafrost. Arct. Antarct. Alp. Res. 47 (1), 71–88.
Panzenböck, M., Mobes-Hansen, B., Albert, R., Herndl, G.J., 2000. Dynamics of phyto- and bacterioplankton in a high Arctic lake on Franz Joseph Land archipelago. Aquat. Microb. Ecol. 21, 265–273.
Petrenko, C.L., Bradley-Cook, J., Lacroix, E.M., Friedland, A.J., Virginia, R.A., 2016. Comparison of carbon and nitrogen storage in mineral soils of graminoid and shrub tundra sites, western Greenland. Arct. Sci. 2, 165–182.
Petrone, J., Sohlenius, G., Johansson, E., Lindborg, T., Näslund, J.-O., Strömgren, M., Brydsten, L., 2016. Using ground-penetrating radar, topography and classification of vegetation to model the sediment and active layer thickness in a periglacial lake catchment, western Greenland. Earth Syst. Sci. Data 8, 663–677.
Pierrot, D., Lewis, E., Wallace, D.W.R., 2006. MS Excel Program Developed for CO2 System Calculations. ORNL/CDIAC-105a: Carbon Dioxide Information Analysis Center, Oak Ridge National Laboratory, U.S. Department of Energy, Oak Ridge, Tennessee.
Presthus Heggen, M., Birks, H.H., Anderson, N.J., 2010. Long-term ecosystem dynamics of a small lake and its catchment in west Greenland. Holocene 20, 1207–1222.
Reimer J., P., Bard, E., Bayliss, A., Beck W., J., Blackwell G., P., Bronk Ramsey, C., Buck E., C., Edwards L., R., Friedrich, M., Grootes M., P., Guliderson P., T., Haflidason, H., Hajdas, I., Hatté, C., Heaton J., T., Hoffmann L., D., Hogg G., A., Hughen A., K., Kaiser F., K., Kromer, B., Manning W., S., Niu, M., Reimer W., R., Richards A., D., Scott M., E., Southon R., J., Turney S.M., C., van der Plicht, J., 2013. IntCal13 and Marine13 radiocarbon age calibration curves, 0-50000 years cal BP. Radiocarbon 55, 1869–1887.
Renberg, I., Hansson, H., 2008. The HTH sediment corer. J. Paleolimnol. 40, 655–659.
Riis, T., Christoffersen, K.S., Baattrup-Pedersen, A., 2016. Mosses in High-Arctic lakes: in situ measurements of annual primary production and decomposition. Polar Biol. 39, 543–552.
Rocher-Ros, G., Giesler, R., Lundin, E., Salimi, S., Jonsson, A., Karlsson, J., 2017. Large lakes dominate CO2 evasion from lakes in an arctic catchment. Geophys. Res. Lett. 44. https://doi.org/10.1002/2017GL076146.
Ruttner-Kolisko, 1977. Suggestions for biomass calculation of plankton rotifers. Arch. Hydrobiol. Beih. Ergebn. Limnol. 8, 71–76.
Rydberg, J., Lindborg, T., Sohlenius, G., Reuss, N., Olsen, J., Laudon, H., 2016. The importance of eolian input on lake-sediment geochemical composition in the dry proglacial landscape of Western Greenland. Arct. Antarct. Alp. Res. 48, 93–109.
Ryves, D.B., McGowan, S., Andersson, N.J., 2002. Development and evaluation of a diatom-conductivity model from lakes in West Greenland. Freshw. Biol. 47, 995–1014.
Sand-Jensen, K., Binzer, T., Middelboe, A.L., 2007. Scaling of photosynthetic production of aquatic macrophytes – a review. Oikos 116, 280–294.
Saros, J.E., Osburn, C.L., Northington, R.M., Birkel, S.D., Auger, J.D., Stedmon, C.A., Anderson, N.J., 2015. Recent decrease in DOC concentrations in Arctic lakes of southwest Greenland. Geophys. Res. Lett. 42, 6703–6709.
Schultz, A.M., 1968. A study of an ecosystem: the arctic tundra. In: Dyne, V.M. (Ed.), The Ecosystem Natural Resource Management. Academic Press, New York, pp. 77–93.
Schuur, E.A.G., Bockheim, J., Canadell, J.G., Euskirchen, E., Field, C.B., Goryachkin, S. V., Hagemann, S., Kuhry, P., Lafleur, P.M., Lee, H., Mazhitova, G., Nelson, F.E., Rinke, A., Romanovsky, V.E., Shiklomanov, N., Tarnocai, C., Venevsky, S., Vogel, J. G., Zimov, S.A., 2008. Vulnerability of permafrost carbon to climate change: Implications for the global carbon cycle. Bioscience 58, 701–714.
Schuur, E.A.G., Vogel, J.G., Crummel, K.G., Lee, H., Sickman, J.O., Osterkamp, T.E., 2009. The effect of permafrost thaw on old carbon release and net carbon exchange from tundra. Nature 459, 556–559.
Shaver, G.R., Chapin, F.S., 1991. Production: biomass relationships and element cycling in contrasting arctic vegetation types. Ecol. Monogr. 61, 1–31.
Siewert, M.B., Hanisch, J., Weiss, N., Kuhry, P., Maximov, T.C., Hugelius, G., 2015. Comparing carbon storage of Siberian tundra and taiga permafrost ecosystems at very high spatial resolution. J. Geophys. Res. Biogeosci. 120, 1973–1994.
Slaymaker, O., 2011. Criteria to distinguish between periglacial, proglacial and paraglacial environments. Quaestiones Geographicae. 30 (1), 85–94.
Smol, J.P., 2012. Climate change: a planet in flux. Nature 483, S12–S15.
Smol, J.P., Douglas, M.S.V., 2007. Crossing the final ecological threshold in high Arctic ponds. PNAS 104, 12395–12397.
Sobek, S., Anderson, N.J., Bernasconi, S.M., Del Sontro, T., 2014. Low organic carbon burial efficiency in arctic lake sediments. J. Geophys. Res. Biogeosci. 119, 1231–1243.
Solomon, C.T., Jones, S.E., Weidel, B.C., Buffam, I., Fork, M.L., Karlsson, J., Larsen, S., Lennon, J.T., Read, J.S., Sadro, S., Saros, J.E., 2015. Ecosystem consequences of changing inputs of terrestrial dissolved organic matter to lakes: current knowledge and future challenges. Ecosystems 18, 376–389. https://doi.org/10.1007/s10021-015-9848-y.
Tang, E.P.Y., Peters, R.H., 1995. The allometry of algal respiration. J. Plankton Res. 17, 303–315.
Tranvik, L.J., Downing, J.A., Cotner, J.B., Loiselle, S.A., Striegl, R.G., Ballatore, T.J., Dillon, P., Finlay, K., Fortino, K., Knoll, L.B., Kortelainen, P.L., Kutser, T., Larsen, S., Laurion, I., Leech, D.M., McCallister, S.L., McKnight, D.M., Melack, J.M., Overholt, E., Porter, J.A., Prairie, Y., Renwick, W.H., Roland, F., Sherman, B.S., Schindler, D. W., Sobek, S., Tremblay, A., Vanni, M.J., Verschoor, A.M., von Wachenfeldt, E., Weyhenmeyer, G.A., 2009. Lakes and reservoirs as regulators of carbon cycling and climate. Limnol. Oceanogr. 54, 2298–2314.
Trumbore, S.E., Harden, J.W., 1997. Accumulation and turnover of carbon in organic and mineral soils of the BOREAS northern study area. J. Geophys. Res.-Atmos. 102, 28817–28830.
Vachon, D., Prairie, Y.T., Cole, J.J., 2010. The relationship between near-surface turbulence and gas transfer velocity in freshwater systems and its implications for floating chamber measurements of gas exchange. Limnol. Oceanogr. 55, 1723–1732.
Vachon, D., Prairie, Y.T., 2013. The ecosystem size and shape dependence of gas transfer velocity versus wind speed relationships in lakes. Can. J. Fish. Aquat. Sci. 70, 1757–1764.
van Bemmelen, J.M., 1890. Über die Bestimmung des Wassers, des Humus, des Schwefels, der in den colloïdalen Silikaten gebundenen Kieselsäure, des Mangans u. s. w. im Ackerboden. Die Landwirthschaftlichen Versuchs-Stationen. 37, 279–290.
van Gool, J., Marker, M., Mengel, F., 1996. The palaeoprotezoic Nagssugtoqidian orogeny in the West Greenland: current status of work by the Danish Lithosphere Centre. Bull. Grønl. Geol. Unders. 172, 88–94.
van Tatenhove, F.G.M., van der Meer, J.J.M., Koster, E.A., 1996. Implications for deglaciation chronology from new AMS age determinations in central west Greenland. Quat. Res. 45 (3), 245–253.
Wanninkhof, R., 2014. Relationship between wind speed and gas exchange over the ocean revisited. Limnol. Oceanogr. Methods 12 (6), 351–362.
Wetzel, R.G., 2001. Limnology: Lake and River Ecosystems. Academic Press, London.
Wetzel, R.G., Likens, G., 1979. Limnological Analyses. W.B. Saunders Co., Philadelphia.
Whalen, S.C., Cornwell, J.C., 1985. Nitrogen, phosphorus, and organic carbon cycling in an arctic lake. Can. J. Fish. Aquat. Sci. 42 (4), 797–808.
Whiteford, E.J., McGowan, S., Barry, C.D., Anderson, N.J., 2016. Seasonal and regional controls of phytoplankton production along a climate gradient in South-West Greenland during ice-cover and ice-free conditions. Arct. Antarct. Alp. Res. 48, 139–159.
Wielgat-Rychert, M., Rychert, K., Witek, Z., Zalewski, M., 2017. Calculation of the photosynthetic quotient (PQ) in the Gulf of Gdańsk (southern Baltic). Baltic Coastal Zone 21, 51–60.
Wielgolaski, F.E., Bliss, L.C., Svobda, J., Doyle, G., 1975. Primary production of tundra. In: Bliss, L.C., Heal, O.W., Moore, J.J. (Eds.), Tundra Ecosystems, - A Comparative Analysis. Cambridge University Press.
Wik, M., Varner, R.K., Anthony, K.W., MacIntyre, S., Bastviken, D., 2016. Climate-sensitive northern lakes and ponds are critical components of methane release. Nat. Geosci. 9, 99–105.
Willemse, N.W., Koster, E.A., Hoogakker, B., van Tatenhove, F.G.M., 2003. A continuous record of Holocene eolian activity in West Greenland. Quat. Res. 59, 322–334.
Young, N.E., Briner, J.P., 2015. Holocene evolution of the western Greenland Ice Sheet: assessing geophysical ice-sheet models with geological reconstructions of ice-marine change. Quat. Sci. Rev. 114, 1–17.